

We are IntechOpen, the world's leading publisher of Open Access books Built by scientists, for scientists

6,900

Open access books available

185,000

International authors and editors

200M

Downloads

Our authors are among the

154

Countries delivered to

TOP 1%

most cited scientists

12.2%

Contributors from top 500 universities



WEB OF SCIENCE™

Selection of our books indexed in the Book Citation Index
in Web of Science™ Core Collection (BKCI)

Interested in publishing with us?
Contact book.department@intechopen.com

Numbers displayed above are based on latest data collected.
For more information visit www.intechopen.com



Topological Interplay between Knots and Entangled Vortex-Membranes

Su-Peng Kou

Additional information is available at the end of the chapter

<http://dx.doi.org/10.5772/intechopen.72809>

Abstract

In this paper, the Kelvin wave and knot dynamics are studied on three dimensional smoothly deformed entangled vortex-membranes in five dimensional space. Owing to the existence of local Lorentz invariance and diffeomorphism invariance, in continuum limit gravity becomes an emergent phenomenon on $3 + 1$ dimensional zero-lattice (a lattice of projected zeroes): on the one hand, the deformed zero-lattice can be denoted by curved space-time for knots; on the other hand, the knots as topological defect of $3 + 1$ dimensional zero-lattice indicates matter may curve space-time. This work would help researchers to understand the mystery in gravity.

Keywords: vortex-membrane, knot, gravity

1. Introduction

A vortex (point-vortex, vortex-line, vortex-membrane) consists of the rotating motion of fluid around a common centerline. It is defined by the vorticity in the fluid, which measures the rate of local fluid rotation. In three dimensional (3D) superfluid (SF), the quantization of the vorticity manifests itself in the quantized circulation $\oint \mathbf{v} \cdot d\mathbf{l} = \frac{h}{m}$ where h is Planck constant and m is atom mass of SF. Vortex-lines can twist around its equilibrium position (common centerline) forming a transverse and circularly polarized wave (Kelvin wave) [1, 2]. Because Kelvin waves are relevant to Kolmogorov-like turbulence [3, 4], a variety of approaches have been used to study this phenomenon. For two vortex-lines, owing to the interaction, the leapfrogging motion has been predicted in classical fluids from the works of Helmholtz and Kelvin [5–10]. Another interesting issue is entanglement between two vortex-lines. In mathematics, vortex-line-entanglement can be characterized by knots with different linking

numbers. The study of knotted vortex-lines and their dynamics has attracted scientists from diverse settings, including classical fluid dynamics and superfluid dynamics [11, 12].

In the paper [13], the Kelvin wave and knot dynamics in high dimensional vortex-membranes were studied, including the leapfrogging motion and the entanglement between two vortex-membranes. A new theory—*knot physics* is developed to characterize the entanglement evolution of 3D leapfrogging vortex-membranes in five-dimensional (5D) inviscid incompressible fluid [13, 14]. According to knot physics, it is the 3D quantum Dirac model that describes the knot dynamics of leapfrogging vortex-membranes (we have called it knot-crystal, that is really plane Kelvin-waves with fixed wave-length). The knot physics may give a complete interpretation on quantum mechanics.

In this paper, we will study the Kelvin wave and knot dynamics on 3D deformed knot-crystal, particularly the topological interplay between knots and the lattice of projected zeroes (we call it zero-lattice). Owing to the existence of local Lorentz invariance and diffeomorphism invariance, the gravitational interaction emerges: on the one hand, the deformed zero-lattice can be denoted by curved space-time; on the other hand, the knots deform the zero-lattice that indicates matter may curve space-time (see below discussion).

The paper is organized as below. In Section 2, we introduce the concept of “zero-lattice” from projecting a knot-crystal. In addition, to characterize the entangled vortex-membranes, we introduce geometric space and winding space. In Section 3, we derive the massive Dirac model in the vortex-representation of knot states on geometric space and that on winding space. In Section 4, we consider the deformed knot-crystal as a background and map the problem onto Dirac fermions on a curved space-time. In Section 5, the gravity in knot physics emerges as a topological interplay between zero-lattice and knots and the knot dynamics on deformed knot-crystal is described by Einstein’s general relativity. Finally, the conclusions are drawn in Section 6.

2. Knot-crystal and the corresponding zero-lattice

2.1. Knot-crystal

Knot-crystal is a system of two periodically entangled vortex-membranes that is described by a special pure state of Kelvin waves with fixed wave length $\mathbf{Z}_{\text{knot-crystal}}(\vec{x}, t)$ [13, 14]. In emergent quantum mechanics, we consider knot-crystal as a ground state for excited knot states, i.e.,

$$\mathbf{Z}_{\text{knot-crystal}}(\vec{x}, t) = \begin{pmatrix} z_A(\vec{x}, t) \\ z_B(\vec{x}, t) \end{pmatrix} \rightarrow |\text{vacuum}\rangle. \quad (1)$$

On the one hand, a knot is a piece of knot-crystal and becomes a topological excitation on it; on the other hand, a knot-crystal can be regarded as a composite system with multi-knot, each of which is described by same tensor state.

Because a knot-crystal is a plane Kelvin wave with fixed wave vector k_0 , we can use the tensor representation to characterize knot-crystals [13],

$$\tilde{\Gamma}_{\text{knot-crystal}}^I = \left(\vec{n}_\sigma^I \sigma^I \right) \otimes \left(\vec{n}_\tau \tau + \vec{1} \tau_0 \right) \quad (2)$$

where $\vec{1} = \begin{pmatrix} 1 & 0 \\ 0 & 1 \end{pmatrix}$ and σ^I, τ^I are 2×2 Pauli matrices for helical and vortex degrees of freedom, respectively. For example, a particular knot-crystal is called SOC knot-crystal $\mathbf{Z}_{\text{knot-crystal}}(\vec{x})$ [13], of which the tensor state is given by

$$\langle \sigma^X \otimes \vec{1} \rangle = \vec{n}_\sigma^X = (1, 0, 0), \langle \sigma^Y \otimes \vec{1} \rangle = \vec{n}_\sigma^Y = (0, 1, 0), \langle \sigma^Z \otimes \vec{1} \rangle = \vec{n}_\sigma^Z = (0, 0, 1). \quad (3)$$

For the SOC knot-crystal, along x -direction, the plane Kelvin wave becomes $z(x) = \sqrt{2}r_0 \cos(k_0 \cdot x)$; along y -direction, the plane Kelvin wave becomes $z(y) = \frac{1}{\sqrt{2}}r_0(e^{ik \cdot y} + ie^{-ik \cdot y})$; along z -direction, the plane Kelvin wave becomes $z(z) = r_0 e^{ik \cdot z}$.

For a knot-crystal, another important property is generalized spatial translation symmetry that is defined by the translation operation $\mathcal{T}(\Delta x^I) = e^{i \cdot (\hat{k}_0^I \cdot \Delta x^I) \cdot \tilde{\Gamma}_{\text{knot-crystal}}^I}$

$$\begin{aligned} \mathbf{Z}(x^I, t) &\rightarrow \mathcal{T}(\Delta x^I) \mathbf{Z}(x^I, t) \\ &= e^{i \cdot (\hat{k}_0^I \cdot \Delta x^I) \cdot \tilde{\Gamma}_{\text{knot-crystal}}^I} \mathbf{Z}(x^I, t). \end{aligned} \quad (4)$$

Here \hat{k}^I is $-i \frac{d}{dx^I}$ ($I = x, y, z$). For example, for the knot states on 3D SOC knot-crystal, the translation operation along x^I -direction becomes

$$\mathcal{T}(\Delta x^I) = e^{i \left(\hat{k}^I \cdot \Delta x^I \right) \cdot (\sigma^I \otimes \vec{1})}. \quad (5)$$

2.2. Winding space and geometric space

For a knot-crystal, we can study its properties on a 3D space (x, y, z) . In the following part, we call the space of (x, y, z) *geometric space*. According to the generalized spatial translation symmetry, each spatial point (x, y, z) in geometric space corresponds to a point denoted by three winding angles $(\Phi_x(x), \Phi_y(y), \Phi_z(z))$ where $\Phi_{x^I}(x^I)$ is the winding angle along x^I -direction. As a result, we may use the winding angles along different directions to denote a given point $\vec{\Phi}(\vec{x}) = (\Phi_x(x), \Phi_y(y), \Phi_z(z))$. We call the space of winding angles $(\Phi_x(x), \Phi_y(y), \Phi_z(z))$ *winding space*. See the illustration in **Figure 1(d)**.

For a 1D leapfrogging knot-crystal that describes two entangled vortex-lines with leapfrogging motion, the function is given by

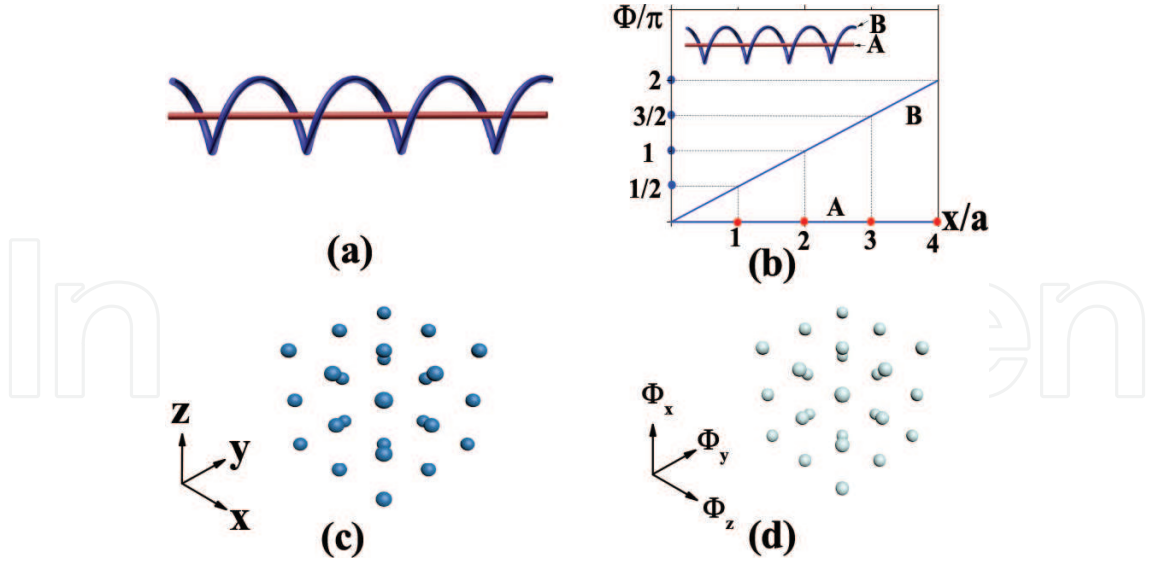


Figure 1. (a) An illustration of a 1D knot-crystal; (b) the relationship between winding angle Φ and coordinate position x . The red dots consist of a 1D zero-lattice in geometric space and the blue dots consist of a zero-lattice in winding space; (c) an illustration of a 3D uniform zero-lattice in geometric space; and (d) an illustration of a 3D uniform zero-lattice in winding space.

$$\mathbf{Z}(\vec{x}, t) = r_0 \begin{pmatrix} \cos\left(\frac{\omega^* t}{2}\right) \\ -i \sin\left(\frac{\omega^* t}{2}\right) \end{pmatrix} e^{i\frac{\pi}{a}x} e^{-i\omega_0 t + i\omega^* t/2}, \quad (6)$$

where ω^* is angular frequency of leapfrogging motion. For the 1D σ_z -knot-crystal, the coordinate on winding space is $\Phi(x) = \frac{\pi}{a}x$. Another example is 3D SOC knot-crystal [10], of which the function is given by

$$\begin{aligned} \mathbf{Z}_{\text{KC}}(\vec{x}, t) &= \begin{pmatrix} \mathbf{Z}_{\text{KC,A}}(\vec{x}, t) \\ \mathbf{Z}_{\text{KC,B}}(\vec{x}, t) \end{pmatrix} = r_0 \begin{pmatrix} \cos\left(\frac{\omega^* t}{2}\right) \\ -i \sin\left(\frac{\omega^* t}{2}\right) \end{pmatrix} e^{-i\omega_0 t + i\omega^* t/2} \\ &\quad \cdot \sqrt{2} r_0 \cos(\Phi_x(x)) \cdot \left(\frac{1}{\sqrt{2}} r_0 \left(e^{i\Phi_y(y)} + i e^{-i\Phi_y(y)} \right) \right) e^{i\Phi_z(z)}, \end{aligned} \quad (7)$$

where the coordinates on winding space are $\Phi_x(x) = \frac{\pi}{a}x$, $\Phi_y(y) = \frac{\pi}{a}y$, $\Phi_z(z) = \frac{\pi}{a}z$, respectively.

In addition, there exists generalized spatial translation symmetry on winding space. On winding space, the translation operation $\mathcal{T}(\Delta\Phi^I)$ becomes

$$\mathcal{T}(\Delta\Phi^I) = e^{i \sum_i \Delta\Phi^I \cdot \vec{\Gamma}_{\text{knot-crystal}}^I} \quad (8)$$

where $\Delta\Phi^I$ denotes the distance on winding space.

2.3. Zero-lattice

Before introduce zero-lattice, we firstly review the projection between two entangled vortex-membranes $z_{A/B}(\vec{x}, t) = \xi_{A/B}(\vec{x}, t) + i\eta_{A/B}(\vec{x}, t)$ along a given direction θ in 5D space by

$$\hat{P}_\theta \begin{pmatrix} \xi_{A/B}(\vec{x}, t) \\ \eta_{A/B}(\vec{x}, t) \end{pmatrix} = \begin{pmatrix} \xi_{A/B, \theta}(\vec{x}, t) \\ [\eta_{A/B, \theta}(\vec{x}, t)]_0 \end{pmatrix} \quad (9)$$

where $\xi_{A/B, \theta}(\vec{x}, t) = \xi_{A/B}(\vec{x}, t) \cos \theta + \eta_{A/B}(\vec{x}, t) \sin \theta$ is variable and $[\eta_{A/B, \theta}(\vec{x}, t)]_0 = \xi_{A/B}(\vec{x}, t) \sin \theta - \eta_{A/B}(\vec{x}, t) \cos \theta$ is constant. So the projected vortex-membrane is described by the function $\xi_{A/B, \theta}(\vec{x}, t)$. For two projected vortex-membranes described by $\xi_{A, \theta}(\vec{x}, t)$ and $\xi_{B, \theta}(\vec{x}, t)$, a zero is solution of the equation

$$\hat{P}_\theta [z_A(\vec{x}, t)] \equiv \xi_{A, \theta}(\vec{x}, t) = \hat{P}_\theta [z_B(\vec{x}, t)] \equiv \xi_{B, \theta}(\vec{x}, t). \quad (10)$$

After projection, the knot-crystal becomes a zero lattice. For example, a 1D leapfrogging knot-crystal is described by

$$z_{KC}(\vec{x}, t) = r_0 \begin{pmatrix} \cos\left(\frac{\omega^* t}{2}\right) \\ -i \sin\left(\frac{\omega^* t}{2}\right) \end{pmatrix} e^{i\frac{\vec{a} \cdot \vec{x}}{a}} e^{-i\omega_0 t + i\omega^* t/2}. \quad (11)$$

According to the knot-equation $\hat{P}_\theta [z_{KC, A}(x)] = \hat{P}_\theta [z_{KC, B}(x)]$, we have

$$\vec{x}_0 = a \cdot X + \frac{a}{\pi} \omega_0 t \quad (12)$$

where $\theta = -\frac{\pi}{2}$ and \vec{x}_0 is the position of zero. As a result, we have a periodic distribution of zeroes (knots).

For a 3D leapfrogging SOC knot-crystal described by $z_{KC}(\vec{x}, t) = \begin{pmatrix} z_{KC, A}(\vec{x}, t) \\ z_{KC, B}(\vec{x}, t) \end{pmatrix}$, we have

similar situation—the solution of zeroes does not change when the tensor order changes, i.e., $\langle \sigma \otimes \vec{1} \rangle = \vec{n}_\sigma = (0, 0, 1) \rightarrow \vec{n}_\sigma = (n_x, n_y, n_x)$ with $|\vec{n}_\sigma| = 1$ [13]. We call the periodic distribution of zeroes to be *zero-lattice*. See the illustration of a 1D zero-lattice in **Figure 1(b)** and 3D zero-lattice in **Figure 1(c)**.

Along a given direction \vec{e} , after shifting the distance a , the phase angle of vortex-membranes in knot-crystal changes π , i.e.,

$$\vec{\Phi}(\vec{x}, t) \rightarrow \vec{\Phi}(\vec{x} + a \cdot \vec{e}, t) = \vec{\Phi}(\vec{x}, t) + \pi. \quad (13)$$

Thus, on the winding space, we have a corresponding “zero-lattice” of discrete lattice sites described by the three integer numbers

$$\vec{X} = (X, Y, Z) = \frac{1}{\pi} \vec{\Phi} - \frac{1}{\pi} \vec{\Phi} \bmod \pi. \quad (14)$$

See the illustration of a 1D zero-lattice in **Figure 1(b)** and 3D zero-lattice in **Figure 1(d)**.

3. Dirac model for knot on zero-lattice

3.1. Dirac model on geometric space

3.1.1. Dirac model in sublattice-representation on geometric space

It was known that in emergent quantum mechanics, a 3D SOC knot-crystal becomes multi-knot system, of which the effective theory becomes a Dirac model in quantum field theory. In emergent quantum mechanics, the Hamiltonian for a 3D SOC knot-crystal has two terms—the kinetic term from global winding and the mass term from leapfrogging motion. Based on a representation of projected state, a 3D SOC knot-crystal is reduced into a “two-sublattice” model with discrete spatial translation symmetry, of which the knot states are described by $|L\rangle$ and $|R\rangle$ (or the Wannier states $c_{L,i}^\dagger |\text{vacuum}\rangle$ and $c_{R,j}^\dagger |\text{vacuum}\rangle$). We call it the Dirac model in *sublattice-representation*.

In sublattice-representation on geometric space, the equation of motion of knots is determined by the Schrödinger equation with the Hamiltonian

$$\begin{aligned} \mathcal{H}_{\text{knot}} &= \int (\psi^\dagger \hat{H}_{\text{knot}} \psi) d^3x, \\ \hat{H}_{\text{knot}} &= -c_{\text{eff}} \vec{\Gamma} \cdot \vec{p}_{\text{knot}} + m_{\text{knot}} c_{\text{eff}}^2 \Gamma^5, \end{aligned} \quad (15)$$

where $\psi^\dagger(t, \vec{x})$ is an four-component fermion field as $\psi^\dagger(t, \vec{x}) = (\psi_{\uparrow L}^\dagger(t, \vec{x}) \ \psi_{\uparrow R}^\dagger(t, \vec{x}) \ \psi_{\downarrow L}^\dagger(t, \vec{x}) \ \psi_{\downarrow R}^\dagger(t, \vec{x}))$. Here, L, R label two chiral-degrees of freedom that denote the two possible sub-lattices, \uparrow, \downarrow label two spin degrees of freedom that denote the two possible winding directions. We have

$$\Gamma^5 = \vec{1} \otimes \iota_x, \quad (16)$$

and

$$\begin{aligned} \Gamma^1 &= \sigma^x \otimes \iota_y, \\ \Gamma^2 &= \sigma^y \otimes \iota_y, \\ \Gamma^3 &= \sigma^z \otimes \iota_y. \end{aligned} \quad (17)$$

$\vec{p}_{\text{knot}} = \hbar_{\text{knot}} \vec{k}$ is the momentum operator. $m_{\text{knot}} c_{\text{eff}}^2 = 2\hbar_{\text{knot}} \omega^*$ plays role of the mass of knots and $c_{\text{eff}} = \frac{aJ}{\hbar_{\text{knot}}} = 2a\omega_0$ play the role of light speed where a is a fixed length that denotes the half pitch of the windings on the knot-crystal.

In addition, the low energy effective Lagrangian of knots on 3D SOC knot-crystal is obtained as

$$\mathcal{L}_{3D} = \bar{\psi} \left(i\gamma^\mu \hat{\partial}_\mu - m_{\text{knot}} \right) \psi \quad (18)$$

where $\bar{\psi} = \psi^\dagger \gamma^0$, γ^μ are the reduced Gamma matrices,

$$\gamma^1 = \gamma^0 \Gamma^1, \gamma^2 = \gamma^0 \Gamma^2, \gamma^3 = \gamma^0 \Gamma^3, \quad (19)$$

and

$$\gamma^0 = \Gamma^5, \gamma^5 = i\gamma^0 \gamma^1 \gamma^2 \gamma^3. \quad (20)$$

3.1.2. Dirac model in vortex-representation on geometric space

In this paper, we derive the effective Dirac model for a knot-crystal based on a representation of vortex degrees of freedom. We call it *vortex-representation*.

In Ref. [13], it was known that a knot has four degrees of freedom, two spin degrees of freedom \uparrow or \downarrow from the helicity degrees of freedom, the other two vortex degrees of freedom from the vortex degrees of freedom that characterize the vortex-membranes, A or B. The basis to define the microscopic structure of a knot is given by $|\uparrow, A\rangle, |\uparrow, B\rangle, |\downarrow, A\rangle, |\downarrow, B\rangle$.

We define operator of knot states by the region of the phase angle of a knot: for the case of $\phi_0 \bmod(2\pi) \in (-\pi, 0]$, we have $c^\dagger|0\rangle$; for the case of $\phi_0 \bmod(2\pi) \in (0, \pi]$, we have $(c^\dagger|0\rangle)^\dagger$. As shown in **Figure 2**, we label the knots by Wannier state $|i, A, \uparrow\rangle, |i+1, A, \uparrow\rangle^*, |i+2, A, \uparrow\rangle, |i+3, A, \uparrow\rangle^* \dots$

To characterize the energy cost from global winding, we use an effective Hamiltonian to describe the coupling between two-knot states along x^l -direction on 3D SOC knot-crystal

$$J c_{A/Bi}^\dagger T_{A/B, A/B}^l c_{A/B, i+e^l} \quad (21)$$

with the annihilation operator of knots at the site i , $c_{A/B, i} = \begin{pmatrix} c_{A/B, \uparrow, i} \\ c_{A/B, \downarrow, i} \end{pmatrix}$. J is the coupling constant between two nearest-neighbor knots. According to the generalized translation symmetry, the transfer matrices $T_{A/B, A/B}^l$ along x^l -direction are defined by

$$T_{A, A}^l = T_{B, B}^l = e^{ia \begin{pmatrix} \hat{k}^l \\ \sigma^l \end{pmatrix}} \quad (22)$$

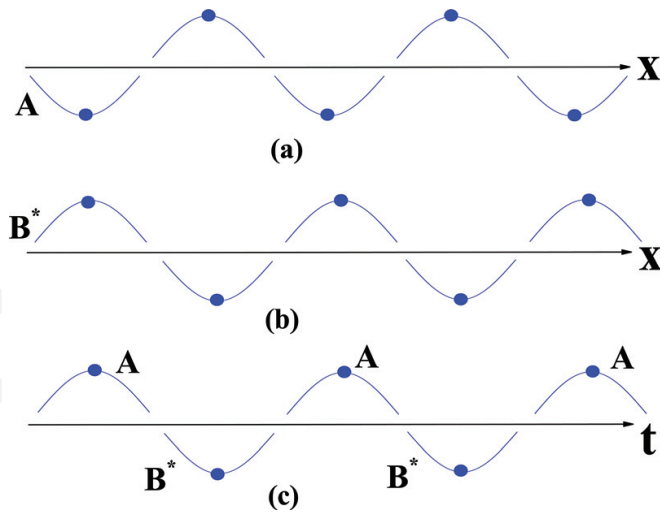


Figure 2. An illustration of knot states in vortex-representation: A and B denote two 1D vortex-lines. Here B^* denotes conjugate representation of vortex-line-B. The curves with blue dots denote knots on the knot-crystal—the curves with blue dot above the line are denoted by $c_i^\dagger|0\rangle$ and the curves with blue dot below the line are denoted by $(c_i^\dagger|0)^\dagger$.

and

$$T_{A,B}^l = T_{B,A}^l = 0. \quad (23)$$

After considering the spin rotation symmetry and the symmetry of vortex-membrane-A and vortex-membrane-B, the effective Hamiltonian from global winding energy can be described by a familiar formulation

$$\mathcal{H}_{\text{coupling}} = \hat{\mathcal{H}}_{\text{coupling},B} + \hat{\mathcal{H}}_{\text{coupling},A} \quad (24)$$

where

$$\hat{\mathcal{H}}_{\text{coupling},A} = J \sum_{i,l} c_{A,i}^\dagger e^{ia \left(\hat{k}^l \cdot \sigma^l \right)} c_{A,i+e^l} + h.c. \quad (25)$$

and

$$\hat{\mathcal{H}}_{\text{coupling},B} = J \sum_{i,l} c_{B,i}^\dagger e^{ia \left(\hat{k}^l \cdot \sigma^l \right)} c_{B,i+e^l} + h.c. \quad (26)$$

We then use path-integral formulation to characterize the effective Hamiltonian for a knot-crystal as

$$\int \mathcal{D}\psi^\dagger(t, \vec{x}) \mathcal{D}\psi(t) e^{i\mathcal{S}/\hbar} \quad (27)$$

where $\mathcal{S} = \int \mathcal{L} dt$ and $\mathcal{L} = i \sum_i \psi_i^\dagger \partial_t \psi_i - \mathcal{H}_{\text{coupling}}$. To describe the knot states on 3D knot-crystal, we have introduced a four-component fermion field to be

$$\psi(\mathbf{x}) = \begin{pmatrix} \psi_{A,\uparrow}(t, \vec{x}) \\ \psi_{B,\uparrow}(t, \vec{x}) \\ \psi_{A,\downarrow}(t, \vec{x}) \\ \psi_{B,\downarrow}(t, \vec{x}) \end{pmatrix} \quad (28)$$

where A, B label vortex degrees of freedom and \uparrow, \downarrow label two spin degrees of freedom that denote the two possible winding directions along a given direction \vec{e} .

In continuum limit, we have

$$\begin{aligned} \mathcal{H}_{\text{coupling}} &= \hat{\mathcal{H}}_{\text{coupling, B}} + \hat{\mathcal{H}}_{\text{coupling, A}} \\ &= 2aJ \sum_k \psi_{A,k}^\dagger [\sigma_x \cos k_x + \sigma_y \cos k_y + \sigma_z \cos k_z] \psi_{A,k} \\ &\quad + 2aJ \sum_k \psi_{B,k}^\dagger [\sigma_x \cos k_x + \sigma_y \cos k_y + \sigma_z \cos k_z] \psi_{B,k} \end{aligned} \quad (29)$$

where the dispersion of knots is

$$E_{A/B,k} \simeq c_{\text{eff}} \left[\left(\vec{k} - \vec{k}_0 \right) \cdot \vec{\sigma} \right], \quad (30)$$

where $\vec{k}_0 = (\frac{\pi}{2}, \frac{\pi}{2}, \frac{\pi}{2})$ and $c_{\text{eff}} = 2aJ$ is the velocity. In the following part we ignore \vec{k}_0 .

Next, we consider the mass term from leapfrogging motion, of which the angular frequency ω^* . For leapfrogging motion obtained by [10], the function of the two entangled vortex-membranes at a given point in geometric space is simplified by

$$\begin{pmatrix} z_A(\vec{x}=0, t) \\ z_B(\vec{x}=0, t) \end{pmatrix} = \frac{r_0}{2} \begin{pmatrix} 1 + e^{i\omega^* t} \\ 1 - e^{i\omega^* t} \end{pmatrix}. \quad (31)$$

At $t = 0$, we have $\begin{pmatrix} z_A(\vec{x}, t) \\ z_B(\vec{x}, t) \end{pmatrix} = \begin{pmatrix} 1 \\ 0 \end{pmatrix}$; at $t = \frac{\pi}{\omega^*}$, we have $\begin{pmatrix} z_A(\vec{x}, t) \\ z_B(\vec{x}, t) \end{pmatrix} = \begin{pmatrix} 0 \\ 1 \end{pmatrix}$. The leap-

frogging knot-crystal leads to periodic varied knot states, i.e., at $t = 0$ we have a knot on vortex-membrane-A that is denoted by $|\sigma, A\rangle$; at $t = \frac{\pi}{\omega^*}$ we have a knot on vortex-membrane-B denoted by $|\sigma, B\rangle$. As a result, the leapfrogging motion becomes a global winding along time direction, $|t, A\rangle, |t + \frac{\pi}{\omega^*}, B\rangle, |t + \frac{2\pi}{\omega^*}, A\rangle, |t + \frac{3\pi}{\omega^*}, B\rangle, \dots$ See the illustration of vortex-representation of knot states for knot-crystal in **Figure 2(c)**. After a time period $t = \frac{\pi}{\omega^*}$, a knot state $\phi_A \bmod(2\pi) \in (-\pi, 0]$ turns into a knot state $\phi_B \bmod(2\pi) \in (-\pi, 0]$. Thus, we use the following formulation to characterize the leapfrogging process,

$$\psi_A^\dagger \psi_B^\dagger. \quad (32)$$

After considering the energy from the leapfrogging process, a corresponding term is given by

$$2\hbar_{\text{knot}}\omega^*\psi_A^\dagger\psi_B^\dagger + h.c. \quad (33)$$

From the global rotating motion denoted $e^{-i\omega_0 t}$, the winding states also change periodically. Because the contribution from global rotating motion $e^{-i\omega_0 t}$ is always canceled by shifting the chemical potential, we do not consider its effect.

From above equation, in the limit $|\vec{k}| \rightarrow 0$ we derive low energy effective Hamiltonian as

$$\begin{aligned} \mathcal{H}_{3D} \simeq & 2aJ \sum_k \psi_{A,k}^\dagger (\vec{\sigma} \cdot \vec{k}) \psi_{A,k} \\ & + 2aJ \sum_k \psi_{B,k}^\dagger (\vec{\sigma} \cdot \vec{k}) \psi_{B,k} \\ & + 2\hbar_{\text{knot}}\omega^* \sum_{k,\sigma} \psi_{A,\sigma,k}^\dagger \psi_{B,\sigma,k}^\dagger \end{aligned} \quad (34)$$

$$\begin{aligned} = & c_{\text{eff}} \int \Psi^\dagger \left[\mathcal{T}_z \otimes (\vec{\sigma} \cdot \hat{k}) \right] \Psi d^3x \\ & + m_{\text{knot}} c_{\text{eff}}^2 \int \Psi^\dagger (\tau_x \otimes \vec{1}) \Psi d^3x. \end{aligned} \quad (35)$$

where

$$\Psi(\mathbf{x}) = \begin{pmatrix} \psi_{A,\uparrow}(t, \vec{x}) \\ \psi_{B,\uparrow}^*(t, \vec{x}) \\ \psi_{A,\downarrow}(t, \vec{x}) \\ \psi_{B,\downarrow}^*(t, \vec{x}) \end{pmatrix}. \quad (36)$$

We then re-write the effective Hamiltonian to be

$$\mathcal{H}_{3D} = \int (\Psi^\dagger \hat{H}_{3D} \Psi) d^3x \quad (37)$$

and

$$\hat{H}_{3D} = c_{\text{eff}} \vec{\Gamma} \cdot \vec{p}_{\text{knot}} + m_{\text{knot}} c_{\text{eff}}^2 \Gamma^5 \quad (38)$$

where

$$\begin{aligned} \Gamma^5 &= \tau^x \otimes 1, \Gamma^1 = \vec{\tau}^z \otimes \sigma^x, \\ \Gamma^2 &= \tau^z \otimes \sigma^y, \Gamma^3 = \tau^z \otimes \sigma^z. \end{aligned} \quad (39)$$

$\vec{p} = \hbar_{\text{knot}} \vec{k}$ is the momentum operator. $\Psi^\dagger = (\psi_{A,\uparrow}^*, \psi_{B,\uparrow}, \psi_{A,\downarrow}^*, \psi_{B,\downarrow})$ is the annihilation operator of four-component fermions. $m_{\text{knot}} c_{\text{eff}}^2 = 2\hbar_{\text{knot}} \omega^*$ plays role of the mass of knots and $c_{\text{eff}} = \frac{2a}{\hbar_{\text{knot}}}$ play the role of light speed where a is a fixed length that denotes the half pitch of the windings on the knot-crystal. In the following parts, we set $\hbar_{\text{knot}} = 1$ and $c_{\text{eff}} = 1$.

Due to Lorentz invariance (see below discussion), the geometric space becomes geometric space-time, i.e., $(x, y, z) \rightarrow (x, y, z, t)$. Here, we may consider $\vec{\Gamma}$ and Γ^5 to be *entanglement matrices* along spatial and tempo direction in winding space-time, respectively. A complete set of entanglement matrices $(\vec{\Gamma}, \Gamma^5)$ is called *entanglement pattern*. The coordinate transformation along $x/y/z/t$ -direction is characterize by $e^{i\vec{\Gamma} \cdot \vec{k}} \cdot \vec{x}$ and $e^{i\Gamma^5 \cdot \hat{\omega}} t$, respectively. Now, the knot becomes topological defect of 3 + 1D entanglement—a knot is not only anti-phase changing along arbitrary spatial direction \vec{e} but also becomes anti-phase changing along tempo direction (along tempo direction, a knot switches a knot state $|A/B\rangle$ to another knot state $|B/A\rangle$).

Finally, the low energy effective Lagrangian of 3D SOC knot-crystal is obtained as

$$\begin{aligned} \mathcal{L}_{3D} &= i\Psi^\dagger \partial_t \Psi - \mathcal{H}_{3D} \\ &= \overline{\Psi} \left(i\gamma^\mu \hat{\partial}_\mu - m_{\text{knot}} \right) \Psi \end{aligned} \quad (40)$$

where $\overline{\Psi} = \Psi^\dagger \gamma^0$, γ^μ are the reduced Gamma matrices,

$$\gamma^1 = \gamma^0 \Gamma^1, \gamma^2 = \gamma^0 \Gamma^2, \gamma^3 = \gamma^0 \Gamma^3, \quad (41)$$

and

$$\gamma^0 = \Gamma^5 = \tau_x \otimes 1, \gamma^5 = i\gamma^0 \gamma^1 \gamma^2 \gamma^3. \quad (42)$$

In addition, we point out that there exists intrinsic relationship between the knot states of sublattice-representation and the knot states of vortex-representation

$$\begin{pmatrix} |A\rangle \\ |B\rangle \end{pmatrix} = \mathcal{U} \begin{pmatrix} |L\rangle \\ |R\rangle \end{pmatrix} \quad (43)$$

where $\mathcal{U} = \exp \left[i\pi \begin{pmatrix} 0 & -i \\ i & 0 \end{pmatrix} \right]$. From the sublattice-representation of knot states, the knot-crystal becomes an object with staggered R/L zeroes along $x/y/z$ spatial directions and time direction; From the vortex-representation of knot states, the knot-crystal becomes an object with global winding along $x/y/z$ spatial directions and time direction. See the illustration of knot states of vortex-representation on a knot-crystal in **Figure 2**.

3.1.3. Emergent Lorentz-invariance

We discuss the emergent Lorentz-invariance for knot states on a knot-crystal.

Since the Fermi-velocity c_{eff} only depends on the microscopic parameter J and a , we may regard c_{eff} to be “light-velocity” and the invariance of light-velocity becomes an fundamental principle for the knot physics. The Lagrangian for massive Dirac fermions indicates emergent $\text{SO}(3,1)$ Lorentz-invariance. The $\text{SO}(3,1)$ Lorentz transformations S_{Lor} is defined by

$$S_{\text{Lor}} \gamma^\mu S_{\text{Lor}}^{-1} = \gamma'^\mu \quad (44)$$

($\mu = 0, 1, 2, 3$) and

$$S_{\text{Lor}} \gamma^5 S_{\text{Lor}}^{-1} = \gamma^5. \quad (45)$$

For a knot state with a global velocity \vec{v} , due to $\text{SO}(3,1)$ Lorentz-invariance, we can do Lorentz boosting on (\vec{x}, t) by considering the velocity of a knot,

$$\begin{aligned} t \rightarrow t' &= \frac{t - \vec{x} \cdot \vec{v}}{\sqrt{1 - \vec{v}^2}} \\ \vec{x} \rightarrow \vec{x}' &= \frac{\vec{x} - \vec{v} \cdot t}{\sqrt{1 - \vec{v}^2}}. \end{aligned} \quad (46)$$

We can do non-uniform Lorentz transformation $S_{\text{Lor}}(\vec{x}, t)$ on knot states $\Psi(\vec{x}, t)$. The *inertial reference-frame* for quantum states of the knot is defined under Lorentz boost, i.e.,

$$\Psi(\vec{x}, t) \rightarrow \Psi'(\vec{x}', t') = S_{\text{Lor}} \cdot \Psi(\vec{x}', t'). \quad (47)$$

For a particle-like knot, a uniform wave-function of knot states $\psi(t)$ is

$$\psi(t) = \frac{1}{\sqrt{V}} e^{-i2\omega^* t}. \quad (48)$$

Under Lorentz transformation with small velocity $|\vec{v}|$, this wave-function $\psi(t)$ is transformed into

$$\begin{aligned} \psi(t) &= \frac{1}{\sqrt{V}} e^{-i2\omega^* t} \\ &\rightarrow \psi' = \frac{1}{\sqrt{V}} e^{-i2\omega^* t'} \\ &\simeq \frac{1}{\sqrt{V}} e^{-i2\omega^* t} \exp\left(-i\left(E_{\text{knot}} t - \vec{p}_{\text{knot}} \cdot \vec{x}\right)\right) \end{aligned} \quad (49)$$

where $E_{\text{knot}} \simeq \frac{\vec{p}_{\text{knot}}^2}{2m_{\text{knot}}}$, $\vec{p}_{\text{knot}} \simeq \omega \vec{v}$ and $m_{\text{knot}} c^2 = 2\omega^*$. As a result, we derive a new distribution of knot-pieces by doing Lorentz transformation, that are described by the plane-wave wave-function $\frac{1}{\sqrt{V}} e^{-i2\omega^* t} \exp(-i(E_{\text{knot}} t - \vec{p}_{\text{knot}} \cdot \vec{x}))$. The new wave-function $\frac{1}{\sqrt{V}} \exp(-i(E_{\text{knot}} t - \vec{p}_{\text{knot}} \cdot \vec{x}))$ comes from the Lorentz boosting S_{Lor} .

Noninertial system can be obtained by considering non-uniformly velocities, i.e., $\vec{v} \rightarrow \Delta \vec{v}(\vec{x}, t)$. According to the linear dispersion for knots, we can do local Lorentz transformation on (\vec{x}, t) i.e.,

$$\begin{aligned} t \rightarrow t'(\vec{x}, t) &= \frac{t - \vec{x} \cdot \Delta \vec{v}}{\sqrt{1 - (\Delta \vec{v})^2}}, \\ \vec{x} \rightarrow \vec{x}'(\vec{x}, t) &= \frac{\vec{x} - \Delta \vec{v} \cdot t}{\sqrt{1 - (\Delta \vec{v})^2}}. \end{aligned} \quad (50)$$

We can also do non-uniform Lorentz transformation $S_{\text{Lor}}(\vec{x}, t)$ on knot states $\Psi(\vec{x}, t)$, i.e.,

$$\begin{aligned} \Psi(\vec{x}, t) &\rightarrow \Psi'(\vec{x}'(\vec{x}, t), t'(\vec{x}, t)) \\ &= S_{\text{Lor}}(\vec{x}, t) \cdot \Psi(\vec{x}, t) \end{aligned} \quad (51)$$

where the new wave-functions of all quantum states change following the non-uniform Lorentz transformation $S_{\text{Lor}}(\vec{x}, t)$. It is obvious that there exists intrinsic relationship between noninertial system and curved space-time.

3.2. Dirac model on winding space

In this part, we show the effective Dirac model of knot states on winding space.

The coordinate measurement of zero-lattice on winding space is the winding angles, $\vec{\Phi}$. Along a given direction \vec{e} , after shifting the distance a , the winding angle changes π . The position is determined by two kinds of values: \vec{X} are integer numbers

$$\vec{X} = (X, Y, Z) = \frac{1}{\pi} \vec{\Phi} - \frac{1}{\pi} \vec{\Phi} \bmod \pi \quad (52)$$

and $\vec{\phi}$ denote internal winding angles

$$\vec{\phi} = (\phi_x, \phi_y, \phi_z) = \vec{\Phi} \bmod \pi \quad (53)$$

with $\phi_x, \phi_y, \phi_z \in (0, \pi]$.

Therefore, on winding space, the effective Hamiltonian turns into

$$\hat{H}_{3D} = \vec{\Gamma} \cdot \vec{p}_{\text{knot}} + m_{\text{knot}} \Gamma^5 = \vec{\Gamma} \cdot \vec{p}_{X, \text{knot}} + \vec{\Gamma} \cdot \vec{p}_{\phi, \text{knot}} + m_{\text{knot}} \Gamma^5 \quad (54)$$

where $\vec{p}_X = \frac{1}{a} i \frac{d}{dX}$ and $\vec{p}_\phi = \frac{1}{a} i \frac{d}{d\phi}$. Because of $\phi_j \in (0, \pi]$, quantum number of \vec{p}_ϕ is angular momentum \vec{L}_ϕ and the energy spectra are $\frac{1}{a} |\vec{L}_\phi|$. If we focus on the low energy physics $E \ll \frac{1}{a}$ (or $\vec{L}_\phi = 0$), we may get the low energy effective Hamiltonian as

$$\hat{H}_{3D} \simeq \vec{\Gamma} \cdot \vec{p}_{X, \text{knot}} + m_{\text{knot}} \Gamma^5. \quad (55)$$

We introduce $3 + 1D$ winding space-time by defining four coordinates on winding space, $\Phi = (\vec{\Phi}, \Phi_t)$ where Φ_t is phase changing under time evolution. For a fixed entanglement pattern $(\vec{\Gamma}, \Gamma^5)$, the coordinate transformation along $x/y/z/t$ -direction on winding space-time is given by $e^{i\vec{\Gamma} \cdot \hat{\Phi}}$ and $e^{i\Gamma^5 \cdot \hat{\Phi}}$, respectively.

For low energy physics, the position in $3 + 1D$ winding space-time is $3 + 1D$ zero-lattice of winding space-time labeled by four integer numbers, $\mathbf{X} = (\vec{X}, X_0)$ where

$$\begin{aligned} \vec{X} &= \frac{1}{\pi} \vec{\Phi} - \frac{1}{\pi} \vec{\Phi} \bmod \pi, \\ X_0 &= \frac{1}{\pi} \Phi_t - \frac{1}{\pi} \Phi_t \bmod \pi. \end{aligned} \quad (56)$$

The lattice constant of the winding space-time is always π that will never be changed. As a result, the winding space-time becomes an effective *quantized* space-time. Because of $x_\mu = a \cdot X_\mu$, the effective action on $3 + 1D$ winding space-time becomes

$$\mathcal{S}_{3D} \simeq (a)^4 \sum_{X, Y, Z, X_0} \mathcal{L}_{3D} \quad (57)$$

where

$$\mathcal{L}_{3D} = \bar{\Psi} \left[i \frac{1}{a} (\gamma^\mu) \hat{\partial}_\mu - m_{\text{knot}} \right] \Psi. \quad (58)$$

4. Deformed zero-lattice as curved space-time

In this section, we discuss the knot dynamics on smoothly deformed knot-crystal (or deformed zero-lattice). We point out that to characterize the entanglement evolution, the corresponding Biot-Savart mechanics for a knot on smoothly deformed zero-lattice is mapped to that in quantum mechanics on a curved space-time.

4.1. Entanglement transformation

Firstly, based on a uniform 3D knot-crystal (uniform entangled vortex-membranes), we introduce the concept of “*entanglement transformation (ET)*”.

Under global entanglement transformation, we have

$$\Psi(\vec{x}, t) \rightarrow \Psi'(\vec{x}, t) = \hat{U}_{\text{ET}}(\vec{x}, t) \cdot \Psi(\vec{x}, t) \quad (59)$$

where

$$\hat{U}_{\text{ET}}(\vec{x}, t) = e^{i\delta\vec{\Phi} \cdot \vec{\Gamma}} \cdot e^{i\delta\Phi_t \cdot \Gamma^5}. \quad (60)$$

Here, $\delta\vec{\Phi}$ and $\delta\Phi_t$ are constant winding angles along spatial $\vec{\Phi}$ -direction and that along tempo direction on geometric space-time, respectively. The dispersion of the excitation changes under global entanglement transformation.

In general, we may define (local) entanglement transformation, i.e.,

$$\hat{U}_{\text{ET}}(\vec{x}, t) = e^{i\delta\vec{\Phi}(\vec{x}, t) \cdot \vec{\Gamma}} \cdot e^{i\delta\Phi_t(\vec{x}, t) \cdot \Gamma^5} \quad (61)$$

where $\delta\vec{\Phi}(\vec{x}, t)$ and $\delta\Phi_t(\vec{x}, t)$ are not constant. We call a system with smoothly varied- $(\delta\vec{\Phi}(\vec{x}, t), \delta\Phi_t(\vec{x}, t))$ *deformed knot-crystal* and its projected zero-lattice *deformed (3 + 1D) zero-lattice*.

4.2. Geometric description for deformed zero-lattice: curved space-time

For knots on a deformed zero-lattice, there exists an intrinsic correspondence between an entanglement transformation $\hat{U}_{\text{ET}}(\vec{x}, t)$ and a local coordinate transformation that becomes a fundamental principle for emergent gravity theory in knot physics.

For zero-lattice, $\hat{U}_{\text{ET}}(\vec{x}, t)$ changes the winding degrees of freedom that is denoted by the local coordination transformation, i.e.,

$$\begin{aligned} \vec{\Phi}(\vec{x}, t) &\Rightarrow \vec{\Phi}'(\vec{x}, t) = \vec{\Phi}(\vec{x}, t) + \delta\vec{\Phi}(\vec{x}, t), \\ \Phi_t(\vec{x}, t) &\Rightarrow \Phi'_t(\vec{x}, t) = \Phi_t(\vec{x}, t) + \delta\Phi_t(\vec{x}, t). \end{aligned} \quad (62)$$

These equations also imply a curved space-time: the lattice constants of the 3 + 1D zero-lattice (the size of a lattice constant with 2π angle changing) are not fixed to be $2a$, i.e.,

$$2a \rightarrow 2a_{\text{eff}}(\vec{x}, t) \quad (63)$$

The distance between two nearest-neighbor “lattice sites” on the spatial/tempo coordinate changes, i.e.,

$$\begin{aligned}\Delta \vec{x} &= (\vec{x} + \vec{e}_x) - \vec{x} = \vec{e}_x, \\ \Delta \vec{x}' &= (\vec{x}' + \vec{e}'_x) - \vec{x}' = \vec{e}'_x(\vec{x}, t)\end{aligned}\quad (64)$$

and

$$\begin{aligned}\Delta t &= (t + e_0) - t = e_0, \\ \Delta t' &= (t' + e'_0) - t' = e'_0(\vec{x}, t)\end{aligned}\quad (65)$$

where $e_a (a = 0, 1, 2, 3)$ and $e'_a(\vec{x}, t)$ are the unit-vectors of the original frame and the deformed frame, respectively. See the illustration of a 1 + 1D deformed zero-lattice on winding space-time with a non-uniform distribution of zeroes in **Figure 3(d)**.

However, for deformed zero-lattice, the information of knots in projected space is invariant: when the lattice-distance of zero-lattice changes $a \rightarrow a_{\text{eff}}(\vec{x}, t)$, the size of the knots correspondingly changes $a \rightarrow a_{\text{eff}}(\vec{x}, t)$. Therefore, due to the invariance of a knot, the deformation of zero-lattice does not change the formula of the low energy effective model for knots on

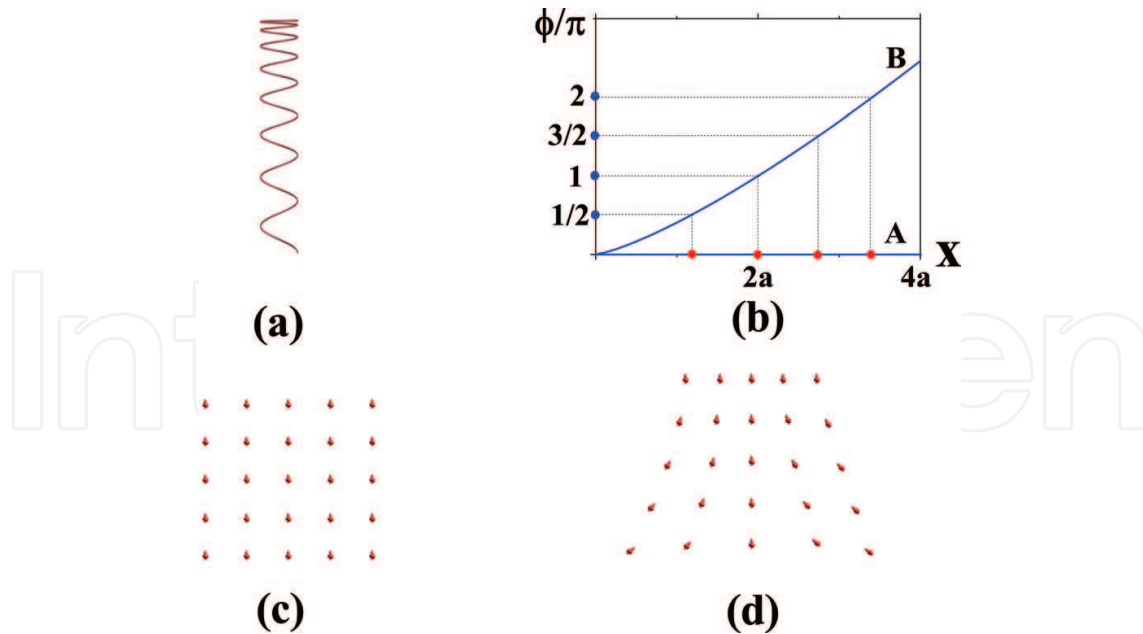


Figure 3. (a) An illustration of deformed knot-crystal; (b) an illustration of smoothly deformed relationship between winding angle Φ and spatial coordinate x . The zero-lattice in winding space is still uniform; while the zero-lattice in geometric space is deformed; (c) an illustration of a uniform 1 + 1D zero-lattice in geometric space-time; and (d) an illustration of a deformed 1 + 1D zero-lattice in geometric space-time.

winding space-time. Because one may smoothly deform the zero-lattice and get the same low energy effective model for knots on winding space-time, there exists *diffeomorphism invariance*, i.e.,

$$\begin{aligned} &\text{Knot-invariance on winding space-time} \\ &\Rightarrow \text{Diffeomorphism invariance.} \end{aligned} \quad (66)$$

Therefore, from the view of mathematics, the physics on winding space-time is never changed! The invariance of the effective model for knots on winding space-time indicates the diffeomorphism invariance

$$S_{\text{zero-lattice}} \equiv (a)^4 \sum_{X, Y, Z, X_0} \bar{\Psi} \left[i \frac{1}{a} \gamma^\mu \hat{\partial}_\mu^X - m_{\text{knot}} \right] \Psi. \quad (67)$$

On the other hand, the condition of very smoothly entanglement transformation guarantees a (local) *Lorentz invariance* in long wave-length limit. Under local Lorentz invariance, the knot-pieces of a given knot are determined by local Lorentz transformations.

According to the local coordinate transformation, the deformed zero-lattice becomes a curved space-time for the knots. In continuum limit $\Delta k \ll (a)^{-1}$ and $\Delta \omega \ll \omega_0$, the diffeomorphism invariance and (local) Lorentz invariance emerge together. E. Witten had made a strong claim about emergent gravity, “*whatever we do, we are not going to start with a conventional theory of non-gravitational fields in Minkowski space-time and generate Einstein gravity as an emergent phenomenon.*” He pointed out that gravity could be emergent only if the notion on the space-time on which diffeomorphism invariance is simultaneously emergent. For the emergent quantum gravity in knot physics, diffeomorphism invariance and Lorentz invariance are simultaneously emergent. In particular, the diffeomorphism invariance comes from information invariance of knots on winding space-time—when the lattice-distance of zero-lattice changes, the size of the knots correspondingly changes.

To characterize the deformed 3 + 1D zero-lattice $(\vec{x}'(\vec{x}, t), t'(\vec{x}, t))$, we introduce a geometric description. In addition to the existence of a set of vierbein fields e^a , the space metric is defined by $\eta_{ab} e_\alpha^a e_\beta^b = g_{\alpha\beta}$ where η is the internal space metric tensor. The geometry fields (vierbein fields $e^a(\vec{x}, t)$ and spin connections $\omega^{ab}(\vec{x}, t)$) are determined by the non-uniform local coordinates $(\vec{x}'(\vec{x}, t), t'(\vec{x}, t))$. Furthermore, one needs to introduce spin connections $\omega^{ab}(\vec{x}, t)$ and the Riemann curvature two-form as

$$\begin{aligned} R_b^a &= d\omega_b^a + \omega_c^a \wedge \omega_b^c \\ &= \frac{1}{2} R_{b\mu\nu}^a dx^\mu \wedge dx^\nu, \end{aligned} \quad (68)$$

where $R_{b\mu\nu}^a \equiv e_\alpha^a e_b^\beta R_{\beta\mu\nu}^\alpha$ are the components of the usual Riemann tensor projection on the tangent space. The deformation of the zero-lattice is characterized by

$$R^{ab} = d\omega^{ab} + \omega^{ac} \wedge \omega^{cb}. \quad (69)$$

So the low energy physics for knots on the deformed zero-lattice turns into that for Dirac fermions on curved space-time

$$\mathcal{S}_{\text{curved-ST}} = \int \sqrt{-g} \bar{\Psi} \left(e_a^\mu \gamma^a \left(i\hat{\partial}_\mu + i\omega_\mu \right) - m_{\text{knot}} \right) \Psi d^4x \quad (70)$$

where $\omega_\mu = \left(\omega_\mu^{0i} \gamma^{0i}/2, \omega_\mu^{ij} \gamma^{ij}/2 \right)$ ($i, j = 1, 2, 3$) and $\gamma^{ab} = -\frac{1}{4} [\gamma^a, \gamma^b]$ ($a, b = 0, 1, 2, 3$) [15]. This model described by $\mathcal{S}_{\text{curved-ST}}$ is invariant under local (non-compact) $\text{SO}(3,1)$ Lorentz transformation $S(\vec{x}, t) = e^{\theta_{ab}(\vec{x}, t) \gamma^{ab}}$ as

$$\begin{aligned} \Psi(\vec{x}, t) &\rightarrow \Psi'(\vec{x}, t) = S(\vec{x}, t) \Psi(\vec{x}, t), \\ \gamma^\mu &\rightarrow \left(\gamma^\mu(\vec{x}, t) \right)' = S(\vec{x}, t) \gamma^\mu \left(S(\vec{x}, t) \right)^{-1}, \\ \omega_\mu &\rightarrow \omega'_\mu(\vec{x}, t) = S(\vec{x}, t) \omega_\mu(\vec{x}, t) \left(S(\vec{x}, t) \right)^{-1} \\ &\quad + S(\vec{x}, t) \partial_\mu \left(S(\vec{x}, t) \right)^{-1}. \end{aligned} \quad (71)$$

γ^5 is invariant under local $\text{SO}(3,1)$ Lorentz symmetry as

$$\begin{aligned} \gamma^5 &\rightarrow (\gamma^5)' = S(\vec{x}, t) \gamma^5 \left(S(\vec{x}, t) \right)^{-1} \\ &= \gamma^5. \end{aligned} \quad (72)$$

In general, an $\text{SO}(3,1)$ Lorentz transformation $S(\vec{x}, t)$ is a combination of spin rotation transformation $\hat{R}(\vec{x}, t) = \hat{R}_{\text{spin}}(\vec{x}, t) \cdot \hat{R}_{\text{space}}(\vec{x}, t)$ and Lorentz boosting $S_{\text{Lor}}(\vec{x}, t)$.

In physics, under a Lorentz transformation, a distribution of knot-pieces changes into another distribution of knot-pieces. For this reason, the velocity c_{eff} and the total number of zeroes N_{knot} are invariant,

$$c_{\text{eff}} \rightarrow c'_{\text{eff}} \equiv c_{\text{eff}} \quad (73)$$

and

$$N_{\text{knot}} \rightarrow N'_{\text{knot}} \equiv N_{\text{knot}}. \quad (74)$$

4.3. Gauge description for deformed zero-lattice

4.3.1. Deformed entanglement matrices and deformed entanglement pattern

The deformation of the zero-lattice leads to deformation of entanglement pattern, i.e.,

$$(\vec{\Gamma}, \Gamma^5) \rightarrow (\vec{\Gamma}'(\mathbf{x}), (\Gamma^5)'(\mathbf{x})) \quad (75)$$

where

$$\vec{\Gamma}'(\mathbf{x}) = \hat{U}_{\text{ET}}(\mathbf{x}) \vec{\Gamma} \hat{U}_{\text{ET}}(\mathbf{x})^{-1}, (\Gamma^5)'(\mathbf{x}) = \hat{U}_{\text{ET}}(\vec{x}, t) \Gamma^5 \hat{U}_{\text{ET}}(\mathbf{x})^{-1}. \quad (76)$$

\mathbf{x} denotes the space-time position of a site of zero-lattice, (\vec{x}, t) . Each entanglement matrix becomes a unit $\text{SO}(4)$ vector-field on each lattice site. The deformed zero-lattice induced by local entanglement transformation $\hat{U}_{\text{ET}}(\mathbf{x})$ is characterized by four $\text{SO}(4)$ vector-fields (four entanglement matrices) $(\vec{\Gamma}'(\mathbf{x}), (\Gamma^5)'(\mathbf{x}))$. See the illustration of a 2D deformed zero-lattice in **Figure 4(d)**, in which the arrows denote deformed entanglement matrix $(\Gamma^5)'(\mathbf{x})$.

4.3.2. Gauge description for deformed tempo entanglement matrix

Firstly, we study the unit $\text{SO}(4)$ vector-field of deformed tempo entanglement matrix $(\Gamma^5)'(\mathbf{x})$. To characterize $(\Gamma^5)'(\mathbf{x})$, the reduced Gamma matrices γ^μ is defined as

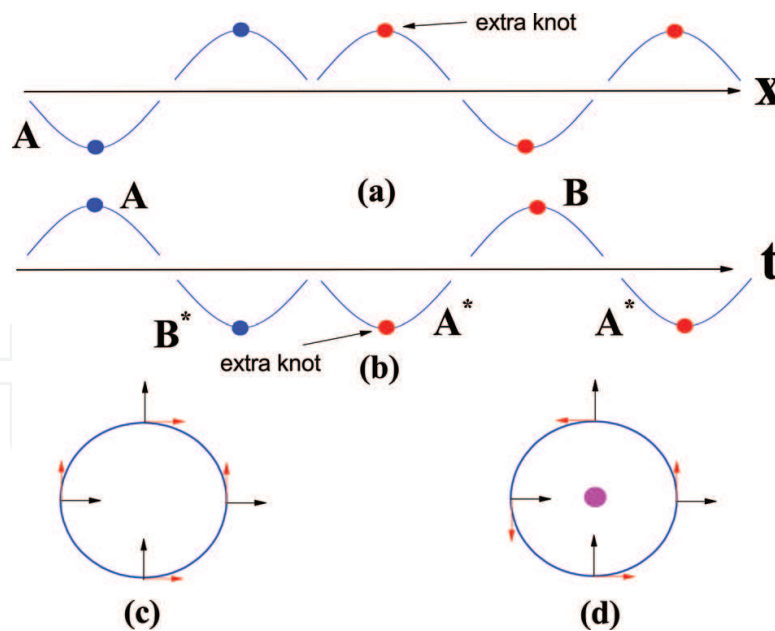


Figure 4. (a) An illustration of the effect of an extra knot on a 1D knot-crystal along spatial direction; (b) an illustration of the effect of an extra knot on a 1D knot-crystal along tempo direction. Here A^*/B^* denotes conjugate representation of vortex-line- A/B ; (c) the entanglement pattern for a uniform knot-crystal. The arrows denote the directions of entanglement matrices; and (d) the entanglement pattern for a knot-crystal with an extra knot at center. The purple spot denotes the knot. The red arrows that denote local tangential entanglement matrices have vortex-like configuration on 2D projected space.

$$\gamma^1 = \gamma^0 \Gamma^1, \gamma^2 = \gamma^0 \Gamma^2, \gamma^3 = \gamma^0 \Gamma^3, \quad (77)$$

and

$$\gamma^0 = \Gamma^5 = \tau^x \otimes 1, \gamma^5 = i\vec{\gamma}^0 \gamma^1 \gamma^2 \gamma^3. \quad (78)$$

Under this definition ($\gamma^0 = \Gamma^5$), the effect of deformed zero-lattice from spatial entanglement transformation $e^{i\Gamma^1 \cdot \Delta\Phi_x}, e^{i\Gamma^2 \cdot \Delta\Phi_y}, e^{i\Gamma^3 \cdot \Delta\Phi_z}$ can be studied due to

$$\Gamma^5 \rightarrow (\Gamma^5)'(\mathbf{x}) = \hat{U}_{\text{ET}}^{x/y/z}(\vec{x}, t) \Gamma^5 \hat{U}_{\text{ET}}^{x/y/z}(\mathbf{x})^{-1} \neq \Gamma^5. \quad (79)$$

However, the effect of deformed zero-lattice from tempo entanglement transformation $e^{i\delta\Phi_t \cdot \Gamma^5}$ cannot be well defined due to

$$\Gamma^5 \rightarrow (\Gamma^5)'(\mathbf{x}) = \hat{U}_{\text{ET}}^t(\vec{x}, t) \Gamma^5 \hat{U}_{\text{ET}}^t(\mathbf{x})^{-1} = \Gamma^5. \quad (80)$$

We introduce an SO(4) transformation $\hat{U}(\vec{x}, t)$ that is a combination of spin rotation transformation $\hat{R}(\mathbf{x})$ and spatial entanglement transformation (entanglement transformation along $x/y/z$ -direction) $\hat{U}_{\text{ET}}^{x/y/z}(\mathbf{x}) = e^{i\delta\Phi(\mathbf{x}) \cdot \vec{\Gamma}}$, i.e.,

$$\hat{U}(\mathbf{x}) = \hat{R}(\mathbf{x}) \oplus \hat{U}_{\text{ET}}^{x/y/z}(\mathbf{x}). \quad (81)$$

Here, \oplus denotes operation combination. Under a non-uniform SO(4) transformation $\hat{U}(\mathbf{x})$, we have

$$\gamma^0 \rightarrow \hat{U}(\mathbf{x}) \gamma^0 (\hat{U}(\mathbf{x}))^{-1} = (\gamma^0(\mathbf{x}))' = \sum_a \gamma^a n^a(\mathbf{x}) \quad (82)$$

where $\mathbf{n} = (n^1, n^2, n^3, \phi_0^0) = (\vec{n}, \phi_0^0)$ is a unit SO(4) vector-field. For the deformed zero-lattice, according to $(\gamma^0(\mathbf{x}))' \neq \gamma^0$, the entanglement matrix $\Gamma^5 = \gamma^0$ along tempo direction is varied, $\Gamma^5 \rightarrow (\Gamma^5)'(\mathbf{x}) \neq \Gamma^5$.

In general, the SO(4) transformation is defined by $\hat{U}(\mathbf{x}) = e^{\Phi_{ab}(\mathbf{x}) \gamma^{ab}}$ ($\gamma^{ab} = -\frac{1}{4}[\gamma^a, \gamma^b]$). Under the SO(4) transformation, we have

$$\begin{aligned} \gamma^\mu &\rightarrow (\gamma^\mu(\mathbf{x}))' = \hat{U}(\mathbf{x}) \gamma^\mu (\hat{U}(\mathbf{x}))^{-1}, \\ A_\mu &\rightarrow A'_\mu(\vec{x}, t) = \hat{U}(\vec{x}, t) A_\mu(\mathbf{x}) (\hat{U}(\mathbf{x}))^{-1} \\ &\quad + \hat{U}(\mathbf{x}) \partial_\mu (\hat{U}(\mathbf{x}))^{-1}. \end{aligned} \quad (83)$$

In particular, γ^5 is invariant under the SO(4) transformation as

$$\gamma^5 \rightarrow (\gamma^5)' = \widehat{U}(\mathbf{x}) \gamma^5 \left(\widehat{U}(\mathbf{x}) \right)^{-1} = \gamma^5. \quad (84)$$

The correspondence between index of γ^a and index of space-time x^a is

$$\begin{aligned} \gamma^1 &\Leftrightarrow x, \gamma^2 \Leftrightarrow y, \\ \gamma^3 &\Leftrightarrow z, \gamma^0 \Leftrightarrow t. \end{aligned} \quad (85)$$

We denote this correspondence to be

$$(1, 2, 3, 0)_{\text{ET}} \Leftrightarrow (1, 2, 3, 0)_{\text{ST}} \quad (86)$$

where $(1, 2, 3, 0)_{\text{ET}}$ denotes the index order of γ^a and $(1, 2, 3, 0)_{\text{ST}}$ denotes the index order of space-time x^a .

As a result, we can introduce an auxiliary gauge field $A_\mu^{ab}(\mathbf{x})$ and use a gauge description to characterize the deformation of the zero-lattice. The auxiliary gauge field $A_\mu^{ab}(\mathbf{x})$ is written into two parts [15]: SO(3) parts

$$A^{ij}(\mathbf{x}) = \text{tr} \left(\gamma^{ij} \left(\widehat{U}(\mathbf{x}) \right) d \left(\widehat{U}(\mathbf{x}) \right)^{-1} \right) \quad (87)$$

and SO(4)/SO(3) parts

$$\begin{aligned} A^{i0}(\mathbf{x}) &= \text{tr} \left(\gamma^{i0} \widehat{U}(\mathbf{x}) \right) d \left(\widehat{U}(\mathbf{x}) \right)^{-1} \\ &= \gamma^0 d(\gamma^i(\mathbf{x}))' = -\gamma^i d(\gamma^0(\mathbf{x}))'. \end{aligned} \quad (88)$$

The total field strength $\mathcal{F}^{ij}(\mathbf{x})$ of $i, j = 1, 2, 3$ components can be divided into two parts

$$\mathcal{F}^{ij}(\mathbf{x}) = F^{ij} + A^{i0} \wedge A^{j0}. \quad (89)$$

According to pure gauge condition, we have Maurer-Cartan equation,

$$\mathcal{F}^{ij}(\mathbf{x}) = F^{ij} + A^{i0} \wedge A^{j0} \equiv 0 \quad (90)$$

or

$$\begin{aligned} F^{ij} &= dA^{ij} + A^{ik} \wedge A^{kj} \\ &\equiv -A^{i0} \wedge A^{j0}. \end{aligned} \quad (91)$$

Finally, we emphasize the equivalence between γ^{0i} and Γ^i , i.e., $\gamma^{0i} \Leftrightarrow \Gamma^i$.

4.3.3. Gauge description for deformed spatial entanglement matrix

Next, we study the unit SO(4) vector-field of deformed spatial entanglement matrix $(\Gamma^i)'(\mathbf{x})$. To characterize $(\Gamma^i)'(\mathbf{x})$, the reduced Gamma matrices γ^μ is defined as

$$\gamma^1 = \gamma^0 \Gamma^j, \gamma^2 = \gamma^0 \Gamma^k, \gamma^3 = \gamma^0 \Gamma^5, \quad (92)$$

and

$$\begin{aligned} \gamma^0 &= \Gamma^i = \tau^z \otimes \sigma^i, \\ \gamma^5 &= i\gamma^0 \gamma^1 \gamma^2 \gamma^3. \end{aligned} \quad (93)$$

Here, Γ^i , Γ^j , and Γ^k are three orthotropic spatial entanglement matrices. Under this definition ($\gamma^0 = \Gamma^i$), the effect of deformed zero-lattice from partial spatial/tempo entanglement transformation $e^{i\Gamma^j \cdot \Delta\Phi_j}$, $e^{i\Gamma^k \cdot \Delta\Phi_k}$, $e^{i\Gamma^5 \cdot \Delta\Phi_t}$ can be studied due to

$$\Gamma^i \rightarrow (\Gamma^i)'(\mathbf{x}) = \hat{U}_{\text{ET}}^{x_j/x_k/t}(\vec{x}, t) \Gamma^i \hat{U}_{\text{ET}}^{x_j/x_k/t}(\mathbf{x})^{-1} \neq \Gamma^i. \quad (94)$$

However, the effect of deformed zero-lattice from spatial entanglement transformation $e^{i\delta\Phi_i \cdot \Gamma^5}$ cannot be well defined due to

$$\Gamma^i \rightarrow (\Gamma^i)'(\mathbf{x}) = \hat{U}_{\text{ET}}^{x_i}(\vec{x}, t) \Gamma^i \hat{U}_{\text{ET}}^{x_i}(\mathbf{x})^{-1} = \Gamma^i. \quad (95)$$

We use similar approach to introduce the gauge description. We can also define the reduced Gamma matrices $\tilde{\gamma}^\mu$ as

$$\tilde{\gamma}^1 = \tilde{\gamma}^0 \Gamma^2, \tilde{\gamma}^2 = \tilde{\gamma}^0 \Gamma^3, \tilde{\gamma}^3 = \tilde{\gamma}^0 \Gamma^5, \quad (96)$$

and

$$\begin{aligned} \tilde{\gamma}^0 &= \Gamma^i = \tau^z \otimes \sigma^x, \\ \tilde{\gamma}^5 &= i\tilde{\gamma}^0 \tilde{\gamma}^1 \tilde{\gamma}^2 \tilde{\gamma}^3. \end{aligned} \quad (97)$$

The correspondence between index of $\tilde{\gamma}^a$ and index of space-time x^a is

$$\begin{aligned} \tilde{\gamma}^1 &\Leftrightarrow y, \tilde{\gamma}^2 \Leftrightarrow z, \\ \tilde{\gamma}^3 &\Leftrightarrow t, \tilde{\gamma}^0 \Leftrightarrow x. \end{aligned} \quad (98)$$

We denote this correspondence to be

$$(1, 2, 3, 0)_{\text{ET}} \Leftrightarrow (2, 3, 0, 1)_{\text{ST}}. \quad (99)$$

Now, the SO(4) transformation $\tilde{U}(\vec{x}, t) = e^{\Phi_{ab}(\vec{x}, t) \tilde{\gamma}^{ab}}$ ($\tilde{\gamma}^{ab} = -\frac{1}{4} [\tilde{\gamma}^a, \tilde{\gamma}^b]$) is not a combination of spin rotation symmetry and entanglement transformation along $x/y/z$ -direction. However, for the case of a or b to be 0, $\tilde{U}(\vec{x}, t) = e^{\Phi_{a0}(\vec{x}, t) \tilde{\gamma}^{a0}}$ denotes the entanglement transformation along $y/z/t$ -direction. The unit SO(4) vector-field on each lattice site becomes

$$\tilde{U}(\mathbf{x})\tilde{\gamma}^0\left(\tilde{U}(\mathbf{x})\right)^{-1} = \left(\tilde{\gamma}^0(\mathbf{x})\right)' = \sum_a \tilde{\gamma}^a \tilde{n}^a(\mathbf{x}) \quad (100)$$

where $\tilde{\mathbf{n}} = (\tilde{n}^1, \tilde{n}^2, \tilde{n}^3, \tilde{\phi}_0^0)$ is a unit vector-field. The auxiliary gauge field $\tilde{A}^{ab}(\mathbf{x})$ are defined by

$$\tilde{A}^{ab}(\mathbf{x}) = \text{tr}\left(\tilde{\gamma}^{ij}\left(\tilde{U}(\mathbf{x})d\left(\tilde{U}(\mathbf{x})\right)^{-1}\right)\right). \quad (101)$$

According to pure gauge condition, we also have the following Maurer-Cartan equation,

$$\tilde{F}^{ij} = d\tilde{A}^{ij} + \tilde{A}^{ik} \wedge \tilde{A}^{kj} \equiv -\tilde{A}^{i0} \wedge \tilde{A}^{j0}. \quad (102)$$

Finally, we emphasize the equivalence between $\tilde{\gamma}^{0i}$ and Γ^a , i.e., $\tilde{\gamma}^{01} \Leftrightarrow \Gamma^2$, $\tilde{\gamma}^{02} \Leftrightarrow \Gamma^3$, $\tilde{\gamma}^{03} \Leftrightarrow \Gamma^5$.

4.3.4. Hidden SO(4) invariant for gauge description

In addition, there exists a hidden global SO(4) invariant for entanglement matrices along different directions in 3 + 1D (winding) space-time $(\vec{\Gamma}, \Gamma^5) \rightarrow (\vec{\Gamma}', (\Gamma^5)')$. To show the hidden SO(4) invariant, we define the reduced Gamma matrices $\tilde{\gamma}^\mu$ as

$$\begin{aligned} \tilde{\gamma}^1 &= \tilde{\gamma}^0 \Gamma^2, \tilde{\gamma}^2 = \tilde{\gamma}^0 \Gamma^3, \tilde{\gamma}^3 = \tilde{\gamma}^0 \Gamma^5, \\ \tilde{\gamma}^0 &= \alpha \Gamma^1 + \beta \Gamma^2 + \gamma \Gamma^3 + \delta \Gamma^5, \\ \tilde{\gamma}^5 &= i\tilde{\gamma}^0 \tilde{\gamma}^1 \tilde{\gamma}^2 \tilde{\gamma}^3 \end{aligned} \quad (103)$$

with $\alpha^2 + \beta^2 + \gamma^2 + \delta^2 = 1$. Here, $\alpha, \beta, \gamma, \delta$ are constant.

Under this description, we can study the entanglement deformation along orthotropic spatial/tempo directions to $x' = \alpha x + \beta y + \gamma z + \delta t$.

4.4. Relationship between geometric description and gauge description for deformed zero-lattice

Due to the generalized spatial translation symmetry there exists an *intrinsic relationship* between gauge description for entanglement deformation between two vortex-membranes and geometric description for global coordinate transformation of the same deformed zero-lattice.

On the one hand, to characterize the changes of the positions of zeroes, we must consider a curved space-time by using geometric description, $\mathbf{x} = (\vec{x}, t) \rightarrow \mathbf{x}' = (\vec{x}', t')$. On the other hand, we need to consider a varied vector-field

$$(\gamma^0(\mathbf{x}))' = \hat{U}(\mathbf{x})\gamma^0(\hat{U}(\mathbf{x}))^{-1} = \sum_a \gamma^a n^a(\mathbf{x}) \quad (104)$$

by using gauge description. There exists intrinsic relationship between the geometry fields $e^a(\mathbf{x})$ ($a = 1, 2, 3, 0$) and the auxiliary gauge fields $A^{a0}(\mathbf{x})$.

For a non-uniform zero-lattice, we have

$$\begin{aligned} \vec{\Phi}(\vec{x}, t) &\Rightarrow \vec{\Phi}'(\vec{x}, t) = \vec{\Phi}(\vec{x}, t) + \delta \vec{\Phi}(\vec{x}, t), \\ \Phi_t(\vec{x}, t) &\Rightarrow \Phi'_t(\vec{x}, t) = \Phi_t(\vec{x}, t) + \delta \Phi_t(\vec{x}, t). \end{aligned} \quad (105)$$

On deformed zero-lattice, the “lattice distances” become dynamic vector fields. We define the vierbein fields $e^a(\mathbf{x})$ that are supposed to transform homogeneously under the local symmetry, and to behave as ordinary vectors under local entanglement transformation along x^a -direction,

$$e^a(\mathbf{x}) = dx^a(\mathbf{x}) = \frac{a}{\pi} d\Phi^a(\mathbf{x}). \quad (106)$$

For the smoothly deformed vector-fields $n^i(\mathbf{x}) \ll 1$, within the representation of $\Gamma^5 = \gamma^0$ we have

$$\begin{aligned} \frac{d\Phi^i(\mathbf{x})}{2\pi} &= n^i(\mathbf{x}) = \text{tr}[\gamma^0 d\gamma^i(\mathbf{x})] \\ &= A^{i0}(\mathbf{x}), i = 1, 2, 3. \end{aligned} \quad (107)$$

Thus, the relationship between $e^i(\mathbf{x})$ and $A^{i0}(\mathbf{x})$ is obtained as

$$e^i(\mathbf{x}) \equiv (2a)A^{i0}(\mathbf{x}). \quad (108)$$

According to this relationship, the changing of entanglement of the vortex-membranes curves the 3D space.

On the other hand, within the representation of $\Gamma^i = \tilde{\gamma}^0$ we have

$$\begin{aligned} \frac{d\Phi^a(\mathbf{x})}{2\pi} &= \tilde{n}^a(\mathbf{x}) = \text{tr}[\tilde{\gamma}^0 d\tilde{\gamma}^a(\mathbf{x})] \\ &= \tilde{A}^{i0}(\mathbf{x}), i = j, k, 0, \end{aligned} \quad (109)$$

and

$$e^0(\mathbf{x}) = dt(\mathbf{x}) = \frac{a}{\pi} d\Phi_t(\mathbf{x}) = (2a)\tilde{A}^{30}(\mathbf{x}). \quad (110)$$

According to this relationship, the changing of entanglement of the vortex-membranes curves the 4D space-time.

In addition, we point out that for different representation of reduced Gamma matrix, there exists intrinsic relationships between the gauge fields $A(\mathbf{x})$ and $\tilde{A}(\mathbf{x})$. After considering these relationships, we have a complete description of the deformed zero-lattice on the geometric space-time,

5. Emergent gravity

Gravity is a natural phenomenon by which all objects attract one another including galaxies, stars, human-being and even elementary particles. Hundreds of years ago, Newton discovered the inverse-square law of universal gravitation, $F = \frac{GMm}{r^2}$ where G is the Newton constant, r is the distance, and M and m are the masses for two objects. One hundred years ago, the establishment of general relativity by Einstein is a milestone to learn the underlying physics of gravity that provides a unified description of gravity as a geometric property of space-time. From Einstein's equations $R_{\mu\nu} - \frac{1}{2}Rg_{\mu\nu} = 8\pi GT_{\mu\nu}$, the gravitational force is really an effect of curved space-time. Here $R_{\mu\nu}$ is the 2nd rank Ricci tensor, R is the curvature scalar, $g_{\mu\nu}$ is the metric tensor, and $T_{\mu\nu}$ is the energy-momentum tensor of matter.

In this section, we point out that there exists emergent gravity for knots on zero-lattice.

5.1. Knots as topological defects

5.1.1. Knot as $SO(4)/SO(3)$ topological defect in $3 + 1D$ space-time

A knot corresponds to an elementary object of a knot-crystal; a knot-crystal can be regarded as composite system of multi-knot. For example, for 1D knot, people divide the knot-crystal into N identical pieces, each of which is just a knot.

From point view of *information*, each knot corresponds to a zero between two vortex-membranes along the given direction. For a knot, there must exist a zero point, at which $\xi_A(x)$ is equal to $\xi_B(x)$. The position of the zero is determined by a local solution of the zero-equation, $F_\theta(x) = 0$ or $\xi_{A,\theta}(x) = \xi_{B,\theta}(x)$.

From point view of *geometry*, a knot (an anti-knot) removes (or adds) a projected zero of zero-lattice that corresponds to removes (or adds) half of "lattice unit" on the zero-lattice according to

$$\Delta x_i = \pm a_{\text{eff}}(\vec{x}, t) \simeq \pm a. \quad (111)$$

As a result, a knot looks like a special type of edge dislocation on $3 + 1D$ zero-lattice. The zero-lattice is deformed and becomes mismatch with an additional knot.

From point view of *entanglement*, a knot becomes topological defect of $3 + 1D$ winding space-time: along x -direction, knot is anti-phase changing denoted by $e^{i\Gamma^1 \cdot \Delta\Phi_x}$, $\Delta\Phi_x = \pi$; along y -direction, knot is anti-phase changing denoted by $e^{i\Gamma^2 \cdot \Delta\Phi_y}$, $\Delta\Phi_y = \pi$; along z -direction, knot

is anti-phase changing denoted by $e^{i\Gamma^3 \cdot \Delta\Phi_z}$, $\Delta\Phi_z = \pi$; along t -direction, knot is anti-phase changing denoted by $e^{i\Gamma^5 \cdot \Delta\Phi_t}$, $\Delta\Phi_t = \pi$. **Figure 4(a) and (b)** shows an illustration a 1D knot.

In mathematics, to generate a knot at (x_0, y_0, z_0, t_0) , we do global topological operation on the knot-crystal, i.e.,

$$e^{i\Gamma^1 \cdot \Delta\Phi_x(\mathbf{x})} |0\rangle \quad (112)$$

with $\Delta\Phi_x = 0, x < x_0$ and $\Delta\Phi_x = \pi, x \geq x_0$;

$$e^{i\Gamma^2 \cdot \Delta\Phi_y(\mathbf{x})} |0\rangle \quad (113)$$

with $\Delta\Phi_y = 0, y < y_0$ and $\Delta\Phi_y = \pi, y \geq y_0$;

$$e^{i\Gamma^3 \cdot \Delta\Phi_z(\mathbf{x})} |0\rangle \quad (114)$$

with $\Delta\Phi_z = 0, z < z_0$ and $\Delta\Phi_z = \pi, z \geq z_0$;

$$e^{i\Gamma^5 \cdot \Delta\Phi_t(\mathbf{x})} |0\rangle \quad (115)$$

with $\Delta\Phi_t = 0, t < t_0$ and $\Delta\Phi_t = \pi, t \geq t_0$. As a result, due to the rotation symmetry in 3 + 1D space-time, a knot becomes $SO(4)/SO(3)$ topological defect. Along arbitrary direction, the local entanglement matrices around a knot at center are switched on the tangential sub-space-time.

5.1.2. Knot as $SO(3)/SO(2)$ magnetic monopole in 3D space

To characterize the topological property of a knot on the 3 + 1D zero-lattice, we use gauge description. We firstly study the tempo entanglement deformation and define $\Gamma^5 = \gamma_0$. Under this gauge description, we can only study the effect of a knot on three spatial zero-lattice.

When there exists a knot, the periodic boundary condition of knot states along arbitrary direction is changed into anti-periodic boundary condition,

$$\Delta\Phi_x = \pi, \Delta\Phi_y = \pi, \Delta\Phi_z = \pi. \quad (116)$$

Consequently, along given direction (for example x -direction), the local entanglement matrices on the tangential sub-space are switched by $e^{i\Gamma^1 \cdot \Delta\Phi_x}$ ($\Delta\Phi_x = \pi$). Along x -direction, in the limit of $x \rightarrow -\infty$, we have the local entanglement matrices on the tangential sub-space as Γ^2 and Γ^3 ; in the limit of $x \rightarrow \infty$, we have the local entanglement matrices on the tangential sub-space as $e^{i\Gamma^1 \cdot \Delta\Phi_x}(\Gamma^2)e^{-i\Gamma^1 \cdot \Delta\Phi_x} = -\Gamma^2$ and $e^{i\Gamma^1 \cdot \Delta\Phi_x}(\Gamma^3)e^{-i\Gamma^1 \cdot \Delta\Phi_x} = -\Gamma^3$.

Because we have similar result along x^i -direction for the system with an extra knot, the system has generalized spatial rotation symmetry. Due to the generalized spatial rotation symmetry, when moving around the knot, the local tangential entanglement matrices (we may use indices j, k to denote the sub space) must rotate synchronously. See the red arrows that denote local

tangential entanglement matrices in **Figure 4(c)** and **(d)**. In **Figure 4(d)**, local tangential entanglement matrices induced by an extra (unified) knot shows vortex-like topological configuration in projected 2D space (for example, x - y plane). As a result, local tangential entanglement matrices induced by an extra knot can be exactly mapped onto that of an orientable sphere with fixed chirality.

To characterize the topological property of 3 + 1D zero-lattice with an extra (unified) knot, we apply gauge description and write down the following constraint

$$\iiint \rho_F dV = \frac{1}{4\pi} \iint \epsilon_{jk} \epsilon_{ijk} F_{jk}^{ik} \cdot dS_i \quad (117)$$

where

$$\begin{aligned} F^{ij} &= dA^{ij} + A^{ik} \wedge A^{kj} \\ &\equiv -A^{i0} \wedge A^{j0} \end{aligned} \quad (118)$$

and $\rho_F = \sqrt{-g} \psi^\dagger \psi$. The upper indices of F_{jk}^{ik} label the local entanglement matrices on the tangential sub-space and the lower indices of F_{jk}^{ik} denote the spatial direction. The non-zero Gaussian integrate $\frac{1}{4\pi} \iint \epsilon_{jk} \epsilon_{ijk} F_{jk}^{ik} \cdot dS_i$ just indicates the local entanglement matrices on the tangential sub-space $A^{i0} \wedge A^{j0}$ to be the local frame of an orientable sphere with fixed chirality.

As a result, the entanglement pattern with an extra 3D knot is topologically deformed and the 3D knot becomes $SO(3)/SO(2)$ magnetic monopole. From the point view of gauge description, a knot traps a “magnetic charge” of the auxiliary gauge field, i.e.,

$$N_F = \int \sqrt{-g} \Psi^\dagger \Psi d^3x = q_m \quad (119)$$

where $q_m = \frac{1}{4\pi} \iint \epsilon_{jk} \epsilon_{ijk} F_{jk}^{ik} \cdot dS_i$ is the “magnetic” charge of auxiliary gauge field A^{ik} . For single knot $N_F = 1$, the “magnetic” charge is $q_m = 1$.

5.1.3. Knot as $SO(3)/SO(2)$ magnetic monopole in 2 + 1D space-time

Next, we study the spatial entanglement deformation and define $\Gamma^i = \tilde{\gamma}_0$. Under this gauge description, we can only study the effect of a knot on 2D spatial zero-lattice and 1D tempo zero-lattice.

In the 2 + 1D space-time, a knot also leads to π -phase changing,

$$\Delta\Phi_i = \pi, \Delta\Phi_j = \pi, \Delta\Phi_t = \pi. \quad (120)$$

Due to the spatial-tempo rotation symmetry, the knot also becomes $SO(3)/SO(2)$ magnetic monopole and traps a “magnetic charge” of the auxiliary gauge field \tilde{A}^{jk} , i.e.,

$$N_F = \int \sqrt{-g} \Psi^\dagger \Psi d^3x = \tilde{q}_m \quad (121)$$

where \tilde{q}_m is the “magnetic” charge of auxiliary gauge field \tilde{A}^{ij} . Remember that the correspondence between index of $\tilde{\gamma}^i$ and index of space-time x^i is $\tilde{\gamma}^1 \Leftrightarrow y, \tilde{\gamma}^2 \Leftrightarrow z, \tilde{\gamma}^3 \Leftrightarrow t$.

To characterize the induced magnetic charge, we write down another constraint

$$\iiint \rho_F dV = \frac{1}{4\pi} \iint \epsilon_{ij} \epsilon_{ijk} \tilde{F}_{jk}^{ij} \cdot dS_i \quad (122)$$

where

$$\begin{aligned} \tilde{F}^{ij} &= d\tilde{A}^{ij} + \tilde{A}^{ij} \wedge \tilde{A}^{ij} \\ &\equiv -\tilde{A}^{i0} \wedge \tilde{A}^{j0}. \end{aligned} \quad (123)$$

The upper indices of $\tilde{F}^{ij} = d\tilde{A}^{ij} + \tilde{A}^{ik} \wedge \tilde{A}^{kj}$ denote the local entanglement matrices on the tangential sub-space-time and the lower indices of \tilde{F}_{jk}^{ij} denote the spatial direction. Therefore, according to above equation, the 2 + 1D zero-lattice is globally deformed by an extra knot.

In general, due to the hidden SO(4) invariant, for other gauge descriptions $\tilde{\gamma}^0 = \alpha\Gamma^1 + \beta\Gamma^2 + \gamma\Gamma^3 + \delta\Gamma^5$, a knot also play the role of SO(3)/SO(2) magnetic monopole and traps a “magnetic charge” of the corresponding auxiliary gauge field.

5.2. Einstein-Hilbert action as topological mutual BF term for knots

It is known that for a given gauge description, a knot is an SO(3)/SO(2) magnetic monopole and traps a “magnetic charge” of the corresponding auxiliary gauge field. For a complete basis of entanglement pattern, we must use four orthotropic SO(4) rotors $((\Gamma^1)'(\mathbf{x}), (\Gamma^2)'(\mathbf{x}), (\Gamma^3)'(\mathbf{x}), (\Gamma^5)'(\mathbf{x}))$ and four different gauge descriptions to characterize the deformation of a knot (an SO(4)/SO(3) topological defect) on a 3 + 1D zero-lattice.

Firstly, we use Lagrangian approach to characterize the deformation of a knot (an SO(3)/SO(2) topological defect) on a 3D spatial zero-lattice, $N_F = q_m$. The topological constraint in Eq. (117) can be re-written into

$$\frac{i}{4} \text{tr} \sqrt{-g} \bar{\Psi} \gamma^i (\gamma^{0i}/2) \Psi = \epsilon_{jk} \epsilon_{ijk} \frac{1}{4\pi} \hat{D}_i F_{jk}^{ik} \quad (124)$$

or

$$\frac{i}{4} \text{tr} \sqrt{-g} \bar{\Psi} \varpi_0^{0i} \gamma^i (\gamma^{0i}/2) \Psi = i \epsilon_{0ijk} \epsilon_{0ijk} \varpi_0^{0i} \frac{1}{4\pi} \hat{D}_i F_{jk}^{ik} \quad (125)$$

where $\hat{D}_i = i\partial_i + i\omega_i$ is covariant derivative in 3 + 1D space-time. ϖ_0^{0i} is a field that plays the role of Lagrangian multiplier. The upper index i of ϖ_0^{0i} denotes the local radial entanglement

matrix around a knot, along which the entanglement matrix does not change. Thus, we use the dual field ϖ^{0i} to enforce the topological constraint in Eq. (117). That is, to denote the upper index of F^{jk} that is the local tangential entanglement matrices, we set antisymmetric property of upper index of ϖ^{0i} and that of F^{jk} . Because ϖ^{0i} and ω^{0i} have the same SO(3,1) generator $(\gamma^{0i}/2)$, due to SO(3,1) Lorentz invariance we can do Lorentz transformation and absorb the dual field ϖ^{0i} into ω^{0i} , i.e., $\omega^{0i} \rightarrow (\omega^{0i})' = \omega^{0i} + \varpi^{0i}$. As a result, the dual field ϖ^{0i} is replaced by ω^{0i} .

In the path-integral formulation, to enforce such topological constraint, we may add a topological mutual BF term S_{MBF1} in the action that is

$$\begin{aligned} S_{\text{MBF1}} &= -\frac{1}{4\pi} \int \epsilon_{0ijk} \epsilon_{0\nu\lambda\kappa} R_{0\nu}^{0i} F_{\lambda\kappa}^{jk} d^4x \\ &= -\frac{1}{4\pi} \int \epsilon_{0ijk} R^{0i} \wedge F^{jk} \end{aligned} \quad (126)$$

where

$$R^{0i} = d\omega^{0i} + \omega^{0j} \wedge \omega^{ji}. \quad (127)$$

From $F^{jk} \equiv -A^{j0} \wedge A^{k0}$ and $e^i \wedge e^j = (2a)^2 A^{j0} \wedge A^{k0}$. The induced topological mutual BF term S_{MBF1} is linear in the conventional strength in R^{0i} and F^{jk} . This term is becomes

$$S_{\text{MBF1}} = \frac{1}{4\pi(2a)^2} \int \epsilon_{0ijk} R^{0i} \wedge e^j \wedge e^k. \quad (128)$$

Next, we use Lagrangian approach to characterize the deformation of a knot (an SO(3)/SO(2) topological defect) on 2 + 1D space-time, $N_F = \tilde{q}_m$. Using the similar approach, we derive another topological mutual BF term S_{MBF2} in the action that is

$$S_{\text{MBF2}} = -\frac{1}{4\pi} \int \epsilon_{0ijk} \epsilon_{0\nu\lambda\kappa} \tilde{R}_{0\nu}^{0i} \tilde{F}_{\lambda\kappa}^{jk} d^4x = -\frac{1}{4\pi} \int \epsilon_{0ijk} \tilde{R}^{0i} \wedge \tilde{F}^{jk} \quad (129)$$

where $\tilde{R}^{0i} = d\tilde{\omega}^{0i} + \tilde{\omega}^{0j} \wedge \tilde{\omega}^{ji}$. From $\tilde{F}^{k0} \equiv -\tilde{A}^{kj} \wedge \tilde{A}^{j0}$ and $\tilde{e}^i \wedge \tilde{e}^j = (2a)^2 \tilde{A}^{j0} \wedge \tilde{A}^{k0}$, this term becomes

$$S_{\text{MBF2}} = \frac{1}{4\pi(2a)^2} \int \epsilon_{ijk0} \tilde{R}^{0i} \wedge \tilde{e}^j \wedge \tilde{e}^k. \quad (130)$$

The upper index of \tilde{R}^{0i} denotes entanglement transformation along given direction in winding space-time. We unify the index order of space-time into $(1, 2, 3, 0)_{\text{ST}}$ and reorganize the upper index. The topological mutual BF term becomes $\frac{1}{4\pi(2a)^2} \int \epsilon_{ijk0} R^{ij} \wedge e^k \wedge e^0$. In Ref. [16–19], a topological description of Einstein-Hilbert action is proposed by S. W. MacDowell and F. Mansouri. The topological mutual BF term proposed in this paper is quite different from the MacDowell-Mansouri action.

According to the diffeomorphism invariance of winding space-time, there exists symmetry between the entanglement transformation along different directions. Therefore, with the help of a complete set of definition of reduced Gamma matrices γ^μ , there exist other topological mutual BF terms $S_{\text{MBF},i}$. For the total topological mutual BF term $S_{\text{MBF}} = \sum_i S_{\text{MBF},i}$ that characterizes the deformation of a knot (an $\text{SO}(4)/\text{SO}(3)$ topological defect) on a 3 + 1D zero-lattice, the upper index of the topological mutual BF term $R^{ij} \wedge e^k \wedge e^l$ must be symmetric, i.e., $i, j, k, l = 1, 2, 3, 0$.

By considering the $\text{SO}(3,1)$ Lorentz invariance, the topological mutual BF term S_{MBF} turns into the Einstein-Hilbert action S_{EH} as

$$\begin{aligned} S_{\text{MBF}} &= S_{\text{EH}} = \frac{1}{16\pi(a)^2} \int \epsilon_{ijkl} R^{ij} \wedge e^k \wedge e^l \\ &= \frac{1}{16\pi G} \int \sqrt{-g} R d^4x \end{aligned} \quad (131)$$

where G is the induced Newton constant which is $G = a^2$. The role of the Planck length is played by $l_p = a$, that is the “lattice” constant on the 3 + 1D zero-lattice.

Finally, from above discussion, we derived an effective theory of knots on deformed zero-lattice in continuum limit as

$$\begin{aligned} S &= S_{\text{zero-lattice}} + S_{\text{EH}} \\ &= \int \sqrt{-g(x)} \bar{\Psi} \left(e_a^\mu \gamma^a \hat{D}_\mu - m_{\text{knot}} \right) \Psi d^4x \\ &\quad + \frac{1}{16\pi G} \int \sqrt{-g} R d^4x \end{aligned} \quad (132)$$

where $\hat{D}_\mu = i\hat{\partial}_\mu + i\omega_\mu$. The variation of the action S via the metric $\delta g_{\mu\nu}$ gives the Einstein's equations

$$R_{\mu\nu} - \frac{1}{2} R g_{\mu\nu} = 8\pi G T_{\mu\nu}. \quad (133)$$

As a result, in continuum limit a knot-crystal becomes a space-time background like smooth manifold with emergent Lorentz invariance, of which the effective gravity theory turns into *topological field theory*.

For emergent gravity in knot physics, an important property is topological interplay between zero-lattice and knots. From the Einstein-Hilbert action, we found that the key property is duality between Riemann curvature R^{ij} and strength of auxiliary gauge field F^{kl} : *the deformation of entanglement pattern leads to the deformation of space-time*.

In addition, there exist a natural energy cutoff $\hbar\omega_0$ and a natural length cutoff a . In high energy limit ($\Delta\omega \sim \omega_0$) or in short range limit ($\Delta x \sim a$), without well-defined 3 + 1D zero-lattice, there does not exist emergent gravity at all.

6. Discussion and conclusion

In this paper, we pointed out that owing to the existence of local Lorentz invariance and diffeomorphism invariance there exists emergent gravity for knots on 3 + 1D zero-lattice. In knot physics, the emergent gravity theory is really a topological theory of entanglement deformation. For emergent gravity theory in knot physics, a topological interplay between 3 + 1D zero-lattice and the knots appears: on the one hand, the deformation of the 3 + 1D zero-lattice leads to the changes of knot-motions that can be denoted by curved space-time; on the other hand, the knots trapping topological defects deform the 3 + 1D zero-lattice that indicates matter may curve space-time. The Einstein-Hilbert action S_{EH} becomes a topological mutual BF term S_{MBF} that exactly reproduces the low energy physics of the general relativity. In **Table 1**, we emphasize the relationship between modern physics and knot physics.

In addition, this work would help researchers to understand the mystery in gravity. In modern physics, matter and space-time are two *different* fundamental objects and matter may move in (flat or curved) space-time. In knot physics, the most important physics idea for gravity is the unification of matter and space-time, i.e.,

$$\text{Matter (knots)} \Leftrightarrow \text{Space-time(zero-lattice)}. \quad (134)$$

One can see that matter (knots) and space-time (zero-lattice) together with motion of matter are *unified* into a simple phenomenon—entangled vortex-membranes and matter (knots) curves space-time (3 + 1D zero-lattice) via a *topological* way.

In the end of the paper, we address the possible physical realization of a 1D knot-crystal based on quantized vortex-lines in ^4He superfluid. Because the emergent gravity in knot physics is topological interplay between zero-lattice and knots, there is no Einstein gravity on a 1D knot-crystal based on entangled vortex-lines in ^4He superfluid. However, the curved space-time could be simulated.

Firstly, we consider two straight vortex-lines in ^4He superfluid between opposite points on the system. Then, we rotate one vortex line around another by a rotating velocity ω_0 . Now, the

Modern physics	Knot physics
Matter	Knot: a topological defect of 3 + 1 D zero-lattice
Motion	Changing of the distribution of knot-pieces
Mass	Angular frequency for leapfrogging motion
Inertial reference system	A knot under Lorentz boosting
Coordinate translation	Entanglement transformation
Space-time	3 + 1D zero-lattice of projected entangled vortex-membranes
Curved space-time	Deformed 3 + 1D zero-lattice
Gravity	Topological interplay between 3 + 1D zero-lattice and knots

Table 1. The relationship between modern physics and knot physics.

winding vortex-line becomes a helical one described by $r_0 e^{ik_0 \cdot x - i\omega_0 t + i\phi_0}$ with $\omega_0 \simeq \left(\frac{\kappa}{4\pi} \ln \frac{1}{k_0 a_0}\right) k_0^2$. As a result, a knot-crystal is realized. For ^4He superfluid, $\kappa = h/m$ is the discreteness of the circulation owing to its quantum nature [2]. h is Planck constant and m is atom mass of SF. So $\kappa = h/m$ is about $10^{-3} \text{ cm}^2/\text{s}$. The length of the half pitch of the windings $a = \frac{\pi}{k_0}$ is set to be 10^{-5} cm , and the distance between two vortex lines r_0 is set to be 10^{-6} cm . We then estimate the effective light speed c_{eff} that is defined by $c_{\text{eff}} = \frac{\kappa k_0}{2\pi} \left(\ln \frac{1}{k_0 a_0} - \frac{1}{2}\right)$ (a_0 denotes the vortex filament radius which is much smaller than any other characteristic size in the system). The effective light speed c_{eff} is about 4 m/s . A non-uniform winding length leads to an effective curved $1 + 1\text{D}$ space-time.

However, at finite temperature, there exist mutual friction and phonon radiation for Kelvin waves on quantized vortex-lines in ^4He superfluid. After considering these dissipation effects, the Kelvin waves are subject to Kolmogorov-like turbulence (even in quantum fluid [3, 4]).

Acknowledgements

This work is supported by NSFC Grant No. 11674026.

Author details

Su-Peng Kou

Address all correspondence to: spkou@bnu.edu.cn

Department of Physics, Beijing Normal University, Beijing, P.R. China

References

- [1] Thomson W. XXIV. Vibrations of a columnar vortex. *Philosophical Magazine*. 1880;**10**:155
- [2] Donnelly RJ. *Quantized Vortices in Helium II*. Cambridge: Cambridge University Press; 1991
- [3] Svistunov BV. Superfluid turbulence in the low-temperature limit. *Physical Review B*. 1995;**52**:3647
- [4] Vinen WF. Classical character of turbulence in a quantum liquid. *Physical Review B*. 2000;**61**:1410
- [5] Dyson FW. The potential of an anchor ring. *Philosophical Transactions of the Royal Society A*. 1893;**184**:1041

- [6] Hicks WM. On the mutual threading of vortex rings. *Proceedings of the Royal Society of London A*. 1922;**102**:111
- [7] Borisov AV, Kilin AA, Mamaev IS. The dynamics of vortex rings: Leapfrogging, choreographies and the stability problem. *Regular and Chaotic Dynamics*. 2013;**18**:33
- [8] Wacks DH, Baggaley AW, Barenghi CF. Coherent laminar and turbulent motion of toroidal vortex bundles. *Physics of Fluids*. 2014;**26**:027102
- [9] Caplan RM, Talley JD, Carretero-González R, Kevrekidis PG. Scattering and leapfrogging of vortex rings in a superfluid. Leapfrogging Kelvin waves, *Physics of Fluids*. 2014;**26**:097101
- [10] Hietala N, Hänninen R, Salman H, Barenghi CF. Leapfrogging Kelvin waves. *arXiv*: 1603.06403
- [11] Kleckner D, Irvine WTM. Creation and dynamics of knotted vortices. *Nature Physics*. 2013;**9**:253
- [12] Hall DS, Ray MW, Tiurev K, Ruokokoski E, Gheorghe AH, Möttönen M. Tying quantum knots. *Nature Physics*. 2016;**12**:478
- [13] Kou SP. Kelvin wave and knot dynamics on entangled vortices. *International Journal of Modern Physics B*. 2017;**31**:1750241
- [14] Kou SP. Knot physics on entangled vortex-membranes: Classification, dynamics and effective theory. *International Journal of Modern Physics B*. 2018;**32**:1850090
- [15] In this paper, we use $I = x, y, z$, $i, j = 1, 2, 3$ and, $a, b = 1, 2, 3, 0$
- [16] MacDowell SW, Mansouri F. Unified geometric theory of gravity and supergravity. *Physical Review Letters*. 1977;**38**:739
- [17] Mansouri F. Superunified theories based on the geometry of local (super-) gauge invariance. *Physical Review D*. 1977;**16**:2456
- [18] Van Nieuwenhuizen P. Supergravity. *Physics Reports*. 1981;**68**:189
- [19] Chamseddine A, West P. Supergravity as a gauge theory of supersymmetry. *Nuclear Physics B*. 1977;**129**:39

